

# Design and Synthesis of Redox Active Diindanes

By

Alex Redmond MacDonald

A thesis submitted to the

Department of Chemistry and Biochemistry

Mount Allison University

in partial fulfillment of the requirements for the

Bachelor of Science degree with Honours

April 2021

# Thesis Committee

---

Supervisor

---

Dr. Glen Briand  
Professor of Chemistry

Reviewer

---

Dr. Steve Westcott  
Professor of Chemistry

## Table of Contents

<b>Thesis Committee.....</b>	<b>1</b>
<b>Acknowledgements .....</b>	<b>4</b>
<b>List of Tables and Figures.....</b>	<b>5</b>
<b>List of Schemes .....</b>	<b>7</b>
<b>List of Spectra in Appendix .....</b>	<b>8</b>
<b>Glossary of Abbreviation and Symbols .....</b>	<b>9</b>
<b>Abstract.....</b>	<b>10</b>
<b>1. Introduction.....</b>	<b>11</b>
<b>1.1 Green Chemistry.....</b>	<b>11</b>
<b>1.2 Catalysis.....</b>	<b>14</b>
<b>1.3 Indium.....</b>	<b>18</b>
<b>1.4 Lewis Acid Indium Catalysts.....</b>	<b>18</b>
<b>1.5 Organoindium Compounds .....</b>	<b>19</b>
<b>1.6 Diindanes .....</b>	<b>21</b>
1.6.1 Stability of Diindanes.....	21
1.6.2 Synthesis of Diindanes .....	22
1.6.3 Reactivity of Diindanes.....	24
<b>1.7 Current Study .....</b>	<b>25</b>
<b>2. Experimental .....</b>	<b>27</b>
<b>2.1 General Methods and Considerations.....</b>	<b>27</b>
2.1.1 Instrumentation.....	27
2.1.2 Reagents .....	27
<b>2.2 Synthesis of C<sub>6</sub>H<sub>3</sub>Br-2,6-(CH<sub>2</sub>Br)<sub>2</sub> (2).....</b>	<b>28</b>
2.2.1 Synthesis of C <sub>6</sub> H <sub>3</sub> Br-2,6-(CH <sub>2</sub> Br) <sub>2</sub> (2) Using Ultraviolet Light.....	28
2.2.2 Synthesis of C <sub>6</sub> H <sub>3</sub> Br-2,6-(CH <sub>2</sub> Br) <sub>2</sub> (2) Using Infrared Light.....	28
<b>2.3 Synthesis of (NCN)Br (3).....</b>	<b>28</b>
<b>2.4 Synthesis of (NCN)InCl<sub>2</sub> (4).....</b>	<b>29</b>
<b>2.5 Attempted Synthesis of [(NCN)InCl]<sub>2</sub>(naphth) (5) .....</b>	<b>29</b>
<b>2.6 Synthesis of Li<sub>2</sub>(naphth)(TMEDA) (7).....</b>	<b>30</b>
<b>2.7 Synthesis of [(NCN)In]<sub>2</sub>(naphth)<sub>2</sub> (8) .....</b>	<b>30</b>
<b>2.8 Attempted Synthesis of [(NCN)InCl]<sub>2</sub> (9) .....</b>	<b>31</b>
<b>3. Results and Discussion.....</b>	<b>32</b>
<b>3.1 Synthesis of C<sub>6</sub>H<sub>3</sub>Br-2,6-(CH<sub>2</sub>Br)<sub>2</sub> (2).....</b>	<b>32</b>
3.1.1 Synthesis of C <sub>6</sub> H <sub>3</sub> Br-2,6-(CH <sub>2</sub> Br) <sub>2</sub> (2) Using Ultraviolet Light .....	32
3.1.2 Synthesis of C <sub>6</sub> H <sub>3</sub> Br-2,6-(CH <sub>2</sub> Br) <sub>2</sub> (2) Using Infrared Light.....	33
<b>3.2 Synthesis of (NCN)Br (3).....</b>	<b>34</b>

3.3 Synthesis of $(\text{NCN})\text{InCl}_2$ (4).....	35
3.4 Attempted Synthesis of $[(\text{NCN})\text{InCl}]_2(\text{naphth})$ (5).....	36
3.5 Synthesis of $\text{Li}_2(\text{naphth})(\text{TMEDA})$ (7).....	37
3.6 Synthesis of $[(\text{NCN})\text{In}]_2(\text{naphth})_2$ (8).....	38
3.7 Attempted Synthesis of $[(\text{NCN})\text{InCl}]_2$ (9).....	40
3.8 X-Ray Crystal Structures.....	41
4. Conclusion .....	44
5. Future Directions .....	45
6. References.....	46
7. Appendix.....	51

## Acknowledgements

I would like to express my deep gratitude to Dr. Briand for his patience and guidance throughout the research and writing process of the thesis you are reading. Without him this work would not have been possible, and I cannot overstate my appreciation for his help over the past year. I would also like to extend my thanks to Dr. Steve Westcott for being my second reader and his help refining this thesis. I would also like to thank my fellow Metalheads, Viv, Alex, and Padma for their help and for making the Metalhead lab such an enjoyable place to work. Special thanks are also extended to Dr. Andrew Grant for his advice regarding ligand prep and for supplying chemicals, as well as Dr. Jason Masuda at Saint Mary's University for the X-ray crystallography analysis.

I would also like to thank Dr. Ralf Brüning for taking a chance on me and allowing me to conduct research with him in the summer of 2019. That summer instilled a love of research in me that remains to this day and his mentorship shaped me into the student that I am today. This research would not have been possible without the help of the Mount Allison staff particularly Phil Cormier, Eva Zhou, Susan Wheaton and Dan Durant. I am deeply appreciative of all the help and training I have received from them. Finally, I would like to thank all the people who have made these past four years so enjoyable and my roommates who made 31 Charlotte St. such a great place to live. I will never forget the impact these people have had on my life and am deeply grateful for them all. Thank you.

Kind regards.

Alex Redmond MacDonald

## List of Tables and Figures

**Figure 1:** The twelve principles of Green Chemistry defined by Anastas and Warner.

**Figure 2:** The catalytic cycle of Wilkinson's catalyst, a rhodium-based catalyst. The intrinsic redox activity of rhodium allows for reversible redox reactions with regeneration of the catalyst at the end of the cycle.

**Figure 3:** The success of indium-based Lewis acid catalysts used in ring opening polymerization reactions highlights the potential of indium compounds as green catalysts. The compound shown contains a chiral salen ligand and outperforms the industry standard catalyst tin (II) octanoate.

**Figure 4:** Oxidation of the In(I) compound  $\eta^5\text{-CpIn}$  to the In(III) compound  $\eta^1\text{-CpInI}_2$ .

**Figure 5:** Disproportionation of the diindane resulting in formation of a In(I) and In(III) species.

**Figure 6:** Pictured is  $(\text{NCN})\text{InCl}_2$ . The ligand NCN stabilizes indane centres through the coordination of a pair of amine groups.

**Figure 7:** Reduction of  $(\text{NCN})\text{InCl}_2$  by the borole reducing agent  $\text{Li}_2[\text{C}_4\text{H}_4\text{BN}(\text{iPr})_2]$  to produce the diindane  $[(\text{NCN})\text{InCl}]_2$ .

**Figure 8:** Formation of the diindane  $[(\text{MeSi})_2(\text{N}^t\text{Bu})_4]\text{In-In}[(\text{N}^t\text{Bu})_4(\text{SiMe})_2]$  through reduction of  $[(\text{MeSi})_2(\text{N}^t\text{Bu})_4]\text{InCl}$  by sodium naphthalide.

**Figure 9:** Synthesis of the diindane  $\text{syn-}[\text{P}_2\text{N}_2]\text{In-In}[\text{P}_2\text{N}_2]$   $[\text{P}_2\text{N}_2 = \text{PhP}(\text{CH}_2\text{SiMe}_2\text{NSiMe}_2\text{CH}_2)_2\text{PPh}]$  through reduction of  $[\text{P}_2\text{N}_2]\text{InCl}$  using the reducing agent potassium graphite.

**Figure 10:** Various isonitriles may be inserted into the diindane with retention of the indium-indium bond to give an In(II) species ( $\text{R} = \text{CMe}_3, \text{C}_6\text{H}_5$ ).

**Figure 11:** Sulfur, selenium, and tellurium may be inserted into the diindane bond by reaction of triethylphosphonium chalcogenides with the In(II) diindane. Products are bent In(III) species with bridging chalcogen atoms between the indium atoms.

**Figure 12:** The target molecule of the study. Each indium atom is in the +2-oxidation state, potentially imparting redox activity to the molecule.

**Figure 13:** The structure of  $[\text{InCl}(\text{pyr})_2]_2(\text{naphth})_2$  as observed by Hoefelmeyer *et al.*

**Figure 14:** X-ray crystal structure of  $(\text{NCN})\text{InBr}_2$  (**6**).

**Figure 15:** X-ray crystal structure of  $[(\text{NCN})\text{In}]_2(\text{naphth})_2$  (**8**). Selected bond distances (Å) and angles (°): In1-C1 = 2.150(9), In1-C11 = 2.170(8), In1-C21 = 2.165(8), In1-N1 = 2.610(8), In1-N2 = 2.568(8), In2-C9 = 2.181(9), In2-C19 = 2.181(9), In2-C33 = 2.21(6), In2-N3 = 2.63(6), In2-N4 = 2.49(2), C1-In1-C11 = 143.4(3), C1-In1-C21 = 109.6(3), C11-In1-C21 = 107.0(3), N1-In1-N2 = 144.8(3), C9-In2-C19 = 143.8(3), C9-In2-C33 = 108.0(8), C19-In2-C33 = 108.2(8), N3-In1-N4 = 141.4(5)

**Table 1:** Comparisons of bond distances (Å) of **8** and  $[\text{InCl}(\text{pyr})_2]_2(\text{naphth})_2$ .

**Table 2:** Comparisons of bond angles (°) of **8** and  $[\text{InCl}(\text{pyr})_2]_2(\text{naphth})_2$ .

## List of Schemes

**Scheme 1:** Synthesis of  $C_6H_3Br-2,6-(CH_2Br)_2$  (**2**) from 2-bromo-*m*-xylene and NBS using ultraviolet light and AIBN to initiate radical reaction.

**Scheme 2:** Synthesis of  $C_6H_3Br-2,6-(CH_2Br)_2$  (**2**) from 2-bromo-*m*-xylene and NBS using infrared light.

**Scheme 3:** Amination of  $C_6H_3Br-2,6-(CH_2Br)_2$  (**2**) to synthesize  $(NCN)Br$  (**3**).

**Scheme 4:** *In situ* generation of  $(NCN)Li$  from  $(NCN)Br$  (**3**) and *n*-butyllithium and subsequent reaction with  $InCl_3$  to form  $(NCN)InCl_2$  (**4**).

**Scheme 5:** Attempted synthesis of  $[(NCN)InCl]_2(naphth)$  (**5**). Attempts to generate  $Li_2(naphth)$  *in situ* and subsequently react it with  $(NCN)InCl_2$  (**4**) were unsuccessful and instead resulted in generation of  $(NCN)InBr_2$  (**6**).

**Scheme 6:** Synthesis of  $Li_2(naphth)(TMEDA)$  (**7**) from 1,8-dibromonaphthalene, *n*-butyllithium, and TMEDA. Though an excess of TMEDA is used per molecule of *n*-butyllithium added,  $^1H$ -NMR shows that only a single TMEDA is bound per molecule of **7**.

**Scheme 7:** Synthesis of  $[(NCN)In]_2(naphth)_2$  (**8**) from  $Li_2(naphth)(TMEDA)$  (**7**) and  $(NCN)InCl_2$  (**4**).

**Scheme 8:** Synthesis of  $[(NCN)InCl]_2$  (**9**) from  $(NCN)InCl_2$  (**4**) using K-Selectride as a reducing agent.

## List of Spectra in Appendix

**Figure A.1:**  $^1\text{H}$ -NMR spectrum in  $\text{CDCl}_3$  of  $\text{C}_6\text{H}_3\text{Br}-2,6-(\text{CH}_2\text{Br})_2$  (**2**) from reaction with ultraviolet light.

**Figure A.2:**  $^1\text{H}$ -NMR spectrum in  $\text{CDCl}_3$  of  $\text{C}_6\text{H}_3\text{Br}-2,6-(\text{CH}_2\text{Br})_2$  (**2**) from reaction with infrared light.

**Figure A.3:**  $^1\text{H}$ -NMR spectrum of  $(\text{NCN})\text{Br}$  (**3**) in  $\text{CDCl}_3$ .

**Figure A.4:**  $^1\text{H}$ -NMR spectrum of  $(\text{NCN})\text{InCl}_2$  (**4**) in  $\text{CDCl}_3$ .

**Figure A.5:**  $^1\text{H}$ -NMR spectrum of  $\text{Li}_2(\text{naphth})(\text{TMEDA})$  (**7**) in  $\text{THF}-d_8$ .

**Figure A.6:**  $^1\text{H}$ -NMR spectrum of  $[(\text{NCN})\text{In}]_2(\text{naphth})_2$  (**8**) in  $\text{CDCl}_3$ .

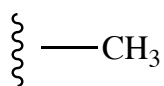
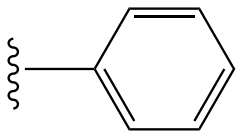
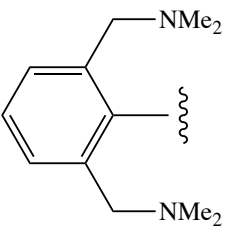
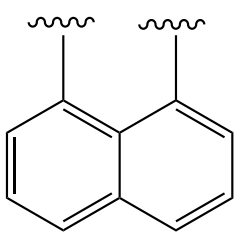
**Figure A.7:**  $^{13}\text{C}\{^1\text{H}\}$ -NMR spectrum of  $[(\text{NCN})\text{In}]_2(\text{naphth})_2$  (**8**) in  $\text{CDCl}_3$ .

**Figure A.8:** FT-IR spectrum of  $[(\text{NCN})\text{In}]_2(\text{naphth})_2$  (**8**).

**Figure A.9:** FT-Raman spectrum of  $[(\text{NCN})\text{In}]_2(\text{naphth})_2$  (**8**).

**Figure A.10:**  $^1\text{H}$ -NMR spectrum of  $[(\text{NCN})\text{InCl}]_2$  (**9**) in  $\text{CDCl}_3$ .

## Glossary of Abbreviation and Symbols

Symbol	Definition	Symbol	Definition
Me	Methyl Group (CH <sub>3</sub> )  	Ph	Phenyl Group (C <sub>6</sub> H <sub>5</sub> )  
NCN	Pincer Ligand [(C <sub>6</sub> H <sub>3</sub> )-2,6-(CH <sub>2</sub> NMe <sub>2</sub> ) <sub>2</sub> ]  	naphth	Naphthalide Ligand (C <sub>10</sub> H <sub>6</sub> )  
THF	Tetrahydrofuran	NBS	<i>N</i> -bromosuccinimide
Et <sub>2</sub> O	Diethyl Ether	AIBN	Azobisisobutyronitrile
CDCl <sub>3</sub>	Deuterated Chloroform	TMEDA	Tetramethylethylenediamine
M	Molarity (mol/L)	In	Indium
mL	Millilitre	<sup>t</sup> Bu	<i>tert</i> -butyl
mmol	Millimole	pyr	Pyridine
NMR	Nuclear Magnetic Resonance	Cp	Cyclopentadienyl
ppm	Parts per million	K-Selectride	Potassium tri( <i>sec</i> -butyl) borohydride
J	Coupling constant		
d	Doublet		
t	Triplet		
m	Multiplet		

## Abstract

The field of Green Chemistry seeks to reduce the risks and environmental impact associated with chemicals and chemical processes. To serve as guidelines for this purposeful design, Anastas and Warner introduced the 12 Principles of Green Chemistry. One of these principles, catalysis, is key as the use of chemical catalysts eliminates waste that would result from the use of stoichiometric amounts of reactant. Many of the most successful and widespread redox catalysts in industry today feature precious heavy transition metals, such as palladium and rhodium, though the toxicity and environmental impact of these metals is undesirable. In contrast to these expensive transition metals, the base main group metal indium possesses several characteristics that make it appealing for green catalysis. Indium compounds are relatively non-toxic and have potential use as Lewis acid catalysts in aqueous solution. Indium is typically trivalent and not intrinsically redox active, which necessitates the design of indium compounds in lowered oxidation states to impart redox activity. The current work seeks to synthesis and characterize the novel redox active diindane  $[(\text{NCN})_2\text{In}_2(\text{naphth})]$  (**1**) which will ultimately be tested as a redox active green catalyst. The synthetic routes explored and the structural characterization of the novel compounds  $(\text{NCN})\text{InBr}_2$  (**6**) and  $[(\text{NCN})\text{In}]_2(\text{naphth})_2$  (**8**) are reported.

# 1. Introduction

## 1.1 Green Chemistry

The concept of Green Chemistry was first articulated in the 1990s and has since become a major area of research. A multitude of programs and government initiatives have followed, all with the purpose of sustainable design.<sup>1</sup> The chemical industry has traditionally been viewed as having harmful effects on both human health and the environment, so much so that the general public has come to associate the term “chemical” with “toxic”. The established practice to reduce risks associated with chemical processes is the creation of rules and regulations regarding circumstantial factors: the use, treatment, and disposal of chemicals.<sup>2</sup> In contrast, Green Chemistry seeks to reduce risk by designing chemicals and processes that are intrinsically less harmful than traditional methods. In other words, chemistry that is “benign by design”.<sup>3</sup> To serve as a guideline for this purposeful design the twelve principles of Green Chemistry were introduced in 1998 by Paul Anastas and John Warner (Figure 1).<sup>1</sup>

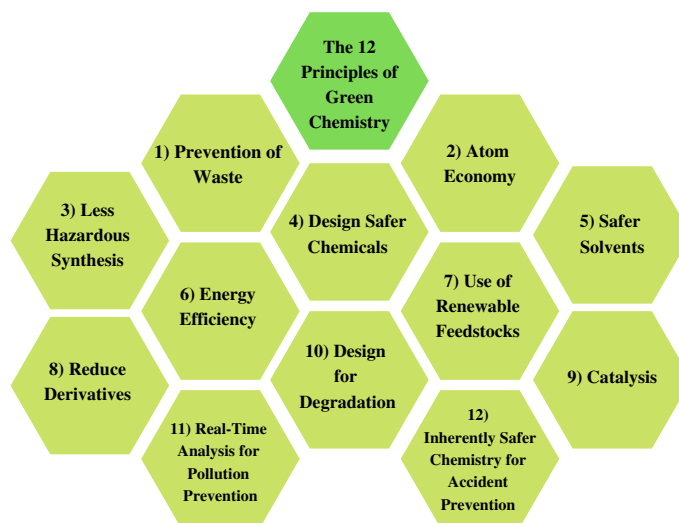


**Figure 1:** The twelve principles of Green Chemistry defined by Anastas and Warner.<sup>1</sup>

These twelve principles of Green Chemistry provide a framework through which existing chemical processes may be critiqued and novel processes designed with conscious attention to their overall environmental impact. This, along with other metrics such as the E-factor developed by Roger Sheldon are used to evaluate the amount of waste produced by a chemical process and emphasize that it is better to prevent production of pollution rather than treat waste.<sup>3</sup>

Development of new pharmaceuticals is a major area of research that has the potential to alleviate human suffering through the development of novel drugs. However, due to the complicated synthetic routes and high purity required in the manufacturing process the pharmaceutical industry produces the highest ratio of waste to product of all of chemical manufacturing sectors.<sup>4,5</sup> Industry's efforts to reduce waste within existing

synthetic routes highlight the effectiveness of the twelve principles of Green Chemistry. For example, the original synthesis for sildenafil citrate (Viagra) required the use of chlorosulfonic acid in a synthetic step after crystallization of an intermediate. The placement of this chlorosulfonation step requires additional purification and multiple solvent exchanges which is both wasteful and energy intensive.<sup>5</sup> The initial linear synthesis was replaced by an improved convergent synthesis which sees the chlorosulfonation step performed prior to crystallization, which purifies the product. The improvements to the synthesis of sildenafil citrate also eliminate the need for the harmful chlorinated solvents and volatile organic solvents originally used. Diethyl ether, chlorinated solvents, methanol and acetone used in the original synthesis are replaced in favour of the greener solvents water and ethyl acetate.<sup>5</sup> This improved synthesis has lowered the solvent waste/ kg product from 1300 L/kg to 7 L/kg, as well as increasing yields of product.<sup>5</sup>

The success of this improved Viagra synthesis shows that through conscious selection of solvents and by designing processes that may be carried out with green solvents one can make existing industrial processes more environmentally friendly as well as more profitable. Pfizer, the manufacturer of sildenafil citrate, recognized these benefits and has developed a series of solvent selection guidelines for medicinal chemistry. These guidelines prioritize safety and environmental impact rather than speed and reliability which are traditionally the only metric on which solvents were judged.<sup>6</sup>

The improved synthesis of Viagra also highlights that through proper implementation of the twelve principles of Green Chemistry both economic and

environmental benefits can be achieved; synergistic effects rather than compromises. It has been found that reducing metrics associated with chemical waste can lower manufacturing costs, and potentially incentivise industry sectors to implement Green Chemistry in their synthetic processes.<sup>3</sup> However, a number of barriers impede wholesale implementation of these Green Chemistry development methods. Current laws tend to punish industries who generate pollution that exceeds a cap rather than rewarding implementation of cleaner processes.<sup>2</sup> Furthermore, if a new green process is found it must have sufficient chemical and economic advantage to warrant the cost to replace the existing system. This replacement must also be able to be implemented quickly to maximize profits within the lifetime of a patent.<sup>2</sup> Despite these challenges Green Chemistry remains a valuable area of research with great potential in the coming decades.

## **1.2 Catalysis**

Of the twelve principles of Green Chemistry, the most pertinent to this study is catalysis. Catalysis is one of the most effective ways of reducing waste in industrial processes as it avoids the need for stoichiometric amounts of reagents.<sup>1</sup> The use of catalysts prevents the generation of stoichiometric amounts of inorganic waste that would otherwise be produced by reactions with elemental metals, metal hydrides, oxides, or acids.<sup>3</sup> The economic and environmental advantages provided by catalysts has led to their widespread adoption in industry, with over 90% of all industrial processes containing a catalytic step.<sup>7</sup>

Another example within the pharmaceutical industry highlights the effectiveness of catalysis in increasing the atom economy of a reaction. Atom economy is a principle that

prioritizes incorporating the maximum amount of atoms from the reactants into the final product.<sup>1</sup> Ibuprofen is a very commonly used over the counter *anti*-inflammatory painkiller. The original synthesis of the drug utilized six steps featuring stoichiometric amounts of reagent and resulted in an atom economy of only 40%. The company BHC designed a new Ibuprofen synthesis featuring three catalytic steps. This improved atom economy to 80% while also managing to recover greater than 99% of the HF catalyst, which can then be reused.<sup>8</sup>

Many of the most successful catalysts currently employed in industry feature transition metals. Precious heavy metals such as palladium, platinum, gold, and rhodium have been mainstays in the field while lighter earth abundant metals such as iron, copper and nickel are receiving increased interest due to their relative abundance and perceived lower toxicity.<sup>9</sup> Several properties of all transition metals make them suitable to use in catalytic transformations. The tendency of transition metal complexes to undergo reversible oxidation state changes and their ability to facilitate  $\pi$ -bond activation, allow them to interact with a variety of common organic functional groups in selective catalytic reactions.<sup>10</sup> The ability of transition metal catalysts to undergo reversible redox reactions and then be regenerated at the end of the catalytic cycle is illustrated in Figure 2 with Wilkinson's catalyst.



ruthenium by-products which can be difficult to remove and require costly and wasteful purification steps.<sup>12</sup> These issues arise in the use of all precious metal catalysts, which has motivated the search for catalysts that are less harmful to human health and therefore have higher levels of acceptable residual metal content.<sup>10</sup>

As well as being toxic to humans, the use of precious transition metals also raises a number of environmental concerns. As the name suggest, these precious transition metals are relatively scarce which causes them to be expensive and unsustainable in the long term. A number of key metals used in catalysts including ruthenium, platinum, palladium, and iridium are considered to be at risk of depletion. Demand for these precious metals has increased in recent years, further accelerating their consumption. As these precious metals deplete from the Earth's crust, the mining process becomes less efficient, which makes it both more wasteful and more expensive.<sup>10</sup> Environmental pollution of platinum group elements from catalytic converters in automobiles is an example of the negative impact these precious transition metals can have. These metals are released during automobile operation and may have negative effects on human health and the environment as the accumulate over time.<sup>13</sup>

As previously mentioned, response to the depletion of precious transition metals has been an increased desire to utilize first row transition metals in catalytic systems. Metals such as nickel, copper, and iron, all of which are traditionally viewed as less toxic, are also more sustainable alternatives than their heavier analogues.<sup>9,10</sup> However, the use of first row transition metals are not without negative environmental impact. Leaching is

observed for all types of catalysts and leads to the release of metal ions into the environment and may cause formation of nanoparticles.<sup>9</sup> These metal by-products are difficult to remove once contamination occurs and represent a clear environmental and health issue. The ideal green catalyst would therefore be benign to both human health and the environment, capable of undergoing reversible redox reactions, and have a cheap, sustainable feedstock.

### **1.3 Indium**

Indium possesses a number of characteristics that make it an appealing choice for use in green catalysts. Indium compounds have been noted for their low toxicity and potential use as Lewis acid catalysts in aqueous solution.<sup>14</sup> Their use in aqueous solution is beneficial as aprotic organic solvents are required in water sensitive processes, though the volatility, flammability, and potential for environmental release of these solvents is undesirable from an environmental perspective.<sup>6</sup> Protic solvents such as water or alcohols, are much greener and the development of catalysts which are tolerant to these solvents is an important aspect of Green Chemistry.<sup>15</sup>

### **1.4 Lewis Acid Indium Catalysts**

As with the other group 13 elements, the most stable oxidation state of indium is +3. Trivalent indium species feature an empty p-orbital that allows the compounds to act as Lewis acids. Indium Lewis acid catalysts have been found to mediate a variety of organic reactions and hold a number of advantages over traditional aluminum Lewis acids, including greater functional group tolerance and reduced sensitivity to water.<sup>16</sup> The use of indium-based Lewis acids in ring opening polymerization reactions illustrates these positive qualities. Numerous indium (III) Lewis acids have been found to catalytically

mediate the polymerization of various cyclic esters with reduced moisture sensitivity and toxicity to their aluminum counterparts. Furthermore, indium-based Lewis acid catalysts, such as the indium-salen complex shown in Figure 3 have been found to be more effective than the industry standard tin (II) octanoate catalyst.<sup>17,18</sup>

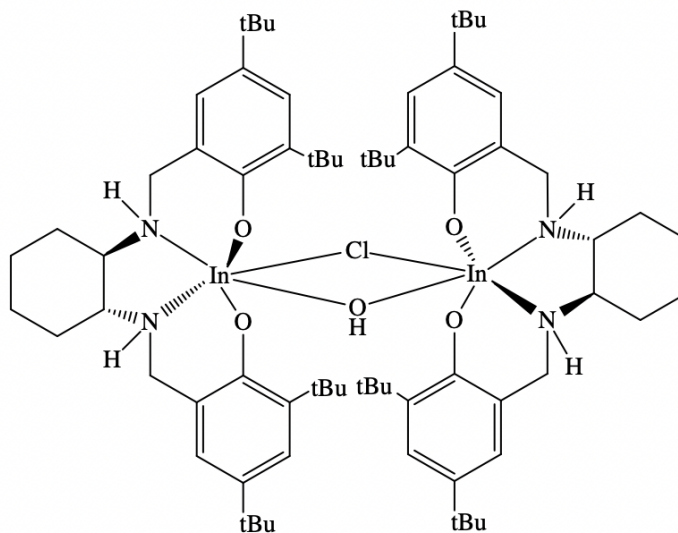


**Figure 3:** The success of indium-based Lewis acid catalysts used in ring opening polymerization reactions highlights the potential of indium compounds as green catalysts. The compound shown contains a chiral salen ligand and outperforms the industry standard catalyst tin (II) octanoate.<sup>18</sup>

### 1.5 Organoindium Compounds

Organoindium compounds are well known in the literature and have found a variety of applications in organic synthesis, with perhaps the most notable being indium mediated allylation reactions.<sup>19</sup> The majority of these organoindium compounds feature indium in the +3 oxidation state, are relatively stable to both air and moisture, and are unreactive to important functional groups such as halides, esters, ketones, and hydroxyl groups.<sup>19</sup> These

qualities make organoindium compounds an attractive choice over other organometallic species whose use would necessitate protection and deprotection of the aforementioned functional groups and greater care to exclude moisture from the reaction. These organoindium compounds and their by-products are also generally less toxic than other organometallic reagents commonly used in organic synthesis.<sup>19</sup>

Though indium-based Lewis acids can be used in catalytic amounts, the applications of redox active organoindium compounds have been mostly limited to use in stoichiometric quantities rather than as catalysts. As indium is not intrinsically redox active, redox activity must be imparted either through the use of redox active ligands or through the design of compounds that feature indium in a lowered oxidation state.<sup>20</sup> Relative to the lighter group 13 analogues, indium has increased stability in oxidation states lower than +3, with many examples of In(I) and In(II) compounds existing in the literature. Indium(I) compounds have been found to undergo oxidation reactions, with the product nearly always being an In(III) species (Figure 4).<sup>20</sup>

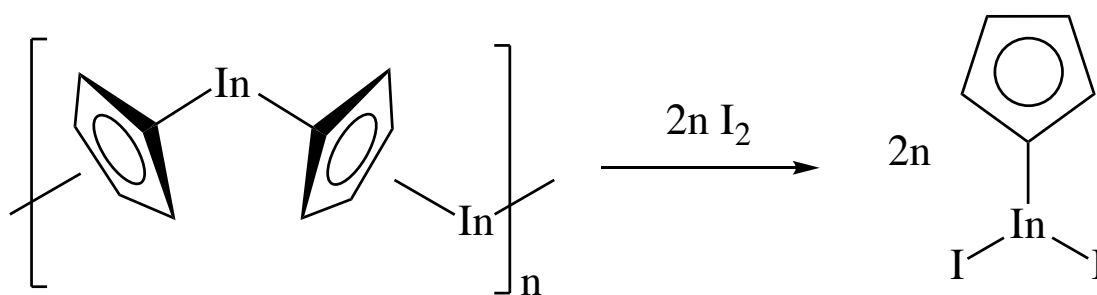


**Figure 4:** Oxidation of the In(I) compound  $\eta^5\text{-CpIn}$  to the In(III) compound  $\eta^1\text{-CpInI}_2$ .<sup>21</sup>

Indium(I) compounds have also been shown to undergo reversible reduction reactions in solution through cyclic voltammetry.<sup>22</sup> Indium(II) compounds are also known to readily undergo oxidation and reduction reactions to the more stable In(I) and In(III) species.<sup>20</sup> The reactivity of these compounds means that mono-nuclear In(II) compounds are not stable under standard conditions.

## 1.6 Diindanes

### 1.6.1 Stability of Diindanes

A well-documented way to synthesize stable In(II) complexes is to design organometallic compounds that feature an indium-indium bond. Pardoe and Downs have compiled a list of diindane compounds in a comprehensive review article on the topic.<sup>20</sup> The diindane bond is weak and must be protected to prevent disproportionation to In(I) and In(III) products. Disproportionation is breakage of the diindane bond that results in disassociation of the two indium atoms (Figure 5).

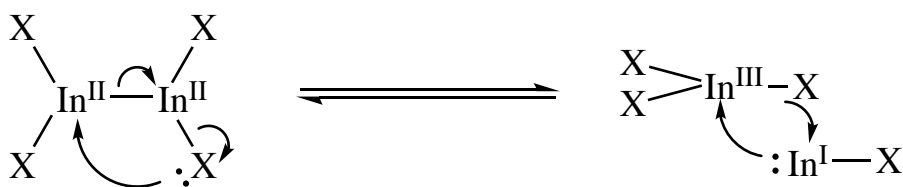


**Figure 5:** Disproportionation of the diindane resulting in formation of a In(I) and In(III) species.<sup>20</sup>

Protection of the diindane bond is achieved either through the use of sterically bulky ligands or polydentate ligands which coordinate to the indium center.<sup>20</sup> When designing

organometallic catalysts, ligands must be carefully chosen as overly bulky ligands will impede formation of the diindane.<sup>18</sup> The ligand  $[(\text{C}_6\text{H}_3)\text{-}2,6\text{-(CH}_2\text{NMe}_2)_2]$  (NCN) has been found to stabilize mononuclear indium compounds through coordination of a pair of amine groups to the metal center (Figure 6). The action of the amine arms chelating to the metal centre has led to this ligand being colloquially referred to as a pincer ligand.<sup>23</sup>

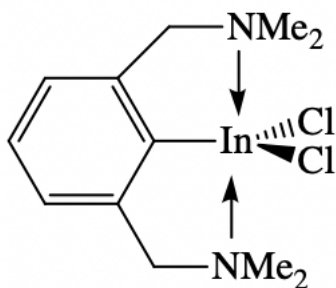


**Figure 6:** Pictured is  $(\text{NCN})\text{InCl}_2$ . The ligand NCN stabilizes indane centres through the coordination of a pair of amine groups.

### 1.6.2 Synthesis of Diindanes

Diindanes may be formed in a number of ways including metathesis reactions with  $\text{In}_2\text{Br}_4$ , reactions with  $\text{In(I)}$  halides, or reduction of trivalent indium species.<sup>20</sup> Reduction of trivalent indium species are of particular interest to the current study. Figure 7 shows the diindane formed from the reduction of  $(\text{NCN})\text{InCl}_2$ . Reduction of indium by the dilithium salt of diisopropylaminoborole results in the formation of a diindane bond which is stabilized by the NCN pincer ligand.<sup>23</sup>

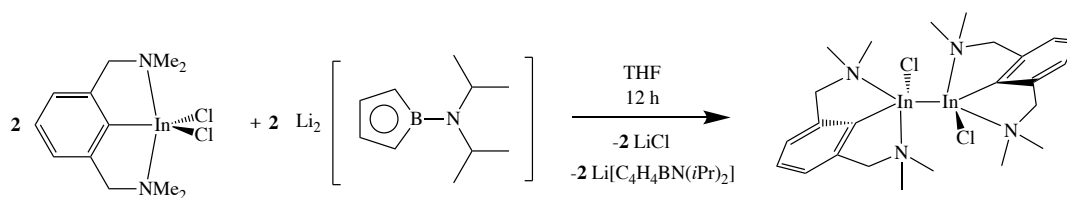


**Figure 7:** Reduction of  $(\text{NCN})\text{InCl}_2$  by the borole reducing agent  $\text{Li}_2[\text{C}_4\text{H}_4\text{BN}(\text{iPr})_2]$  to produce the diindane  $[(\text{NCN})\text{InCl}]_2$ .<sup>23</sup>

Veith *et al.* synthesized the diindane  $[(\text{MeSi})_2(\text{N}^t\text{Bu})_4]\text{In}-\text{In}[(\text{N}^t\text{Bu})_4(\text{SiMe})_2]$  through reduction of  $[(\text{MeSi})_2(\text{N}^t\text{Bu})_4]\text{InCl}$  using the reducing agent sodium naphthalide (Figure 8).<sup>24</sup>

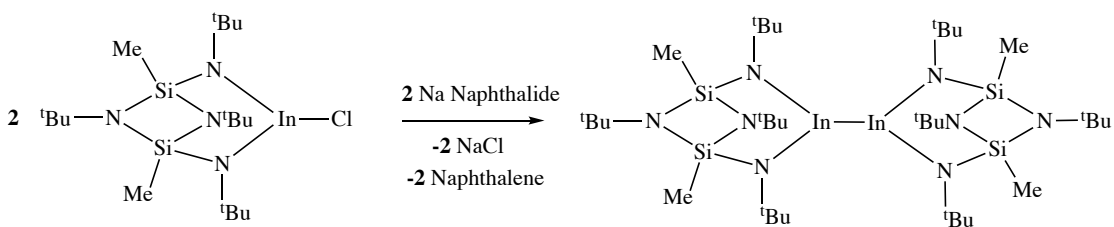


**Figure 8:** Formation of the diindane  $[(\text{MeSi})_2(\text{N}^t\text{Bu})_4]\text{In}-\text{In}[(\text{N}^t\text{Bu})_4(\text{SiMe})_2]$  through reduction of  $[(\text{MeSi})_2(\text{N}^t\text{Bu})_4]\text{InCl}$  by sodium naphthalide.<sup>24</sup>

Fryzuk *et al.* similarly reduces an In(III) compound using potassium graphite as a reducing agent to synthesize the diindane  $\text{syn}-[\text{P}_2\text{N}_2]\text{In}-\text{In}[\text{P}_2\text{N}_2]$  [ $\text{P}_2\text{N}_2 = \text{PhP}(\text{CH}_2\text{SiMe}_2\text{NSiMe}_2\text{CH}_2)_2\text{PPh}$ ] from  $[\text{P}_2\text{N}_2]\text{InCl}$  (Figure 9).<sup>25</sup>

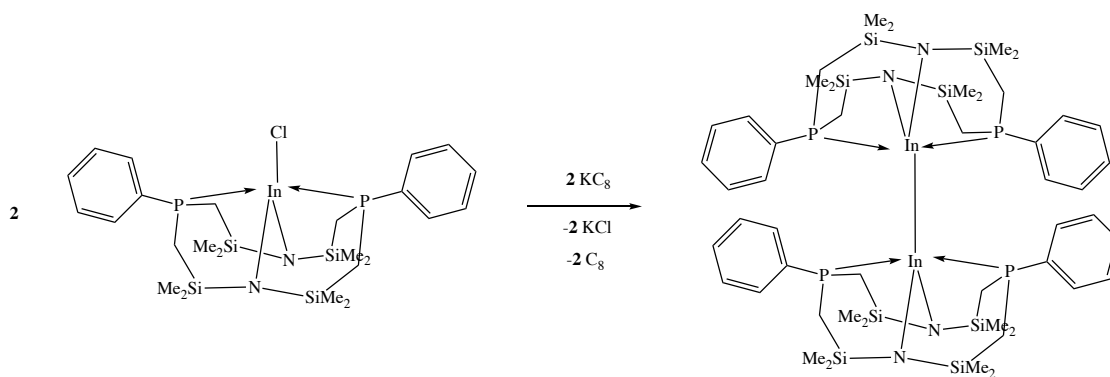


**Figure 9:** Synthesis of the diindane  $\text{syn-[P}_2\text{N}_2\text{]In-In[P}_2\text{N}_2\text{]}$  [ $\text{P}_2\text{N}_2 = \text{PhP}(\text{CH}_2\text{SiMe}_2\text{NSiMe}_2\text{CH}_2)_2\text{PPh}$ ] through reduction of  $[\text{P}_2\text{N}_2]\text{InCl}$  using the reducing agent potassium graphite.<sup>25</sup>

### 1.6.3 Reactivity of Diindanes

Diindane compounds have been found to undergo a variety of redox, addition, and metathesis reactions which may indicate that diindanes have potential as synthetic precursors or catalysts.<sup>20</sup> Diindanes react readily with small molecules as these species may insert or interact with the diindane bond in a redox reaction. Various isonitrile species have been found to form adducts with diindanes to generate In(II) species with retention of the diindium bond (Figure 10).<sup>26</sup>

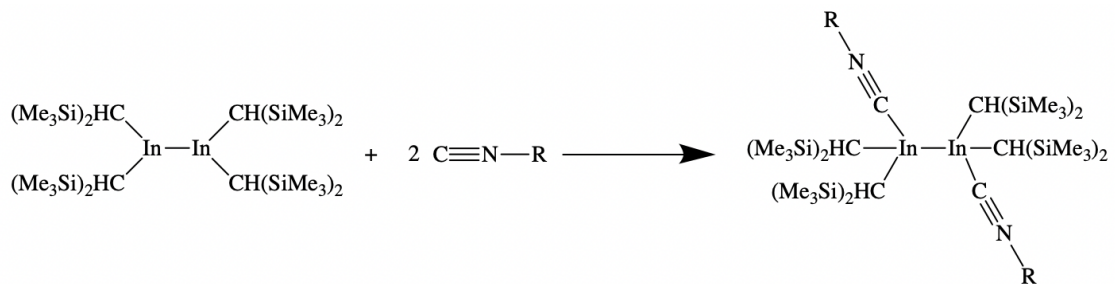


**Figure 10:** Various isonitriles may be inserted into the diindane with retention of the indium-indium bond to give an In(II) species ( $\text{R} = \text{CMe}_3, \text{C}_6\text{H}_5$ ).<sup>26</sup>

The heavier chalcogens have also been found to react with diindanes *via* chalcogen insertion into the indium-indium bond yielding chalcogen bridged dinuclear In(III) compounds (Figure 12).<sup>27</sup>

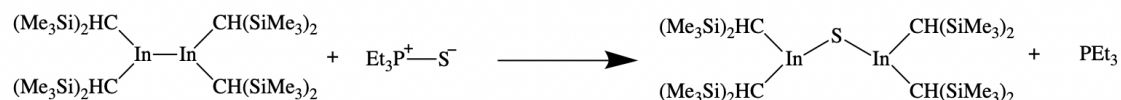


**Figure 11:** Sulfur, selenium, and tellurium may be inserted into the diindane bond by reaction of triethylphosphonium chalcogenides with the In(II) diindane. Products are bent In(III) species with bridging chalcogen atoms between the indium atoms.<sup>27</sup>

Despite their potential, diindane compounds have not found widespread use as they lack the robustness of other organoindium compounds. As outlined previously, the diindane bond is weak and exposure to air and moisture may lead to disproportionation.<sup>20</sup> A further complication is that previously reported oxidative addition reactions with small molecules are not reversible, which leads to diindanes being used in stoichiometric rather than catalytic quantities.<sup>20</sup> To be an effective catalytic system, the diindane molecule must undergo a redox reaction followed by reformation of the indium-indium bond, making the process reversible.

### 1.7 Current Study

The focus of the current study was to synthesize and characterize a novel redox active diindane compound [(NCN)<sub>2</sub>In<sub>2</sub>(naphth)] (**1**) (Figure 12). The chosen ligand to

stabilize the indium centres for the diindane bond is the pincer ligand NCN (Figure 6). The indium atoms of the diindane will also be bridged *via* a 1,8-naphthalene ligand (naphth) so that the close proximity of the two atoms will encourage the reformation of the indium-indium bond after redox reaction. This would therefore make the breaking and subsequent reformation of the bond a reversible process and be a major step towards diindane catalysis. Naphthalene is a desirable bridging ligand as the polyaromatic nature of the compound will maintain a rigid structure and ensure the indium atoms retain the correct bonding geometry. Novel diindanes will be characterized with  $^1\text{H}$  and  $^{13}\text{C}\{^1\text{H}\}$  NMR spectroscopy, elemental analysis, melting point, FT-IR and FT-Raman spectroscopy, and X-ray crystallography. The redox activity of these compounds will be tested with cyclic voltammetry and through oxidation with diphenyl disulfide.

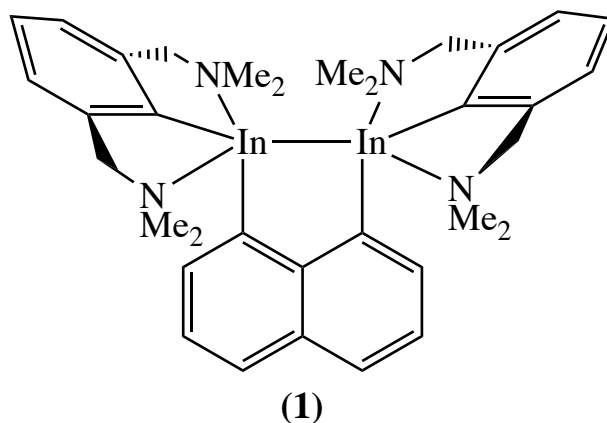


**Figure 12:** The target molecule of the study. Each indium atom is in the +2-oxidation state, potentially imparting redox activity to the molecule.

## 2. Experimental

### 2.1 General Methods and Considerations.

#### 2.1.1 Instrumentation

Air and moisture sensitive reactions were carried out under dinitrogen atmosphere using an Innovative Technology glovebox and standard Schlenk line techniques. NMR spectra was collected using a Varian Mercury 200 MHz+ Spectrometer at 25 °C. Melting point of synthesized compounds was carried out using a Electrothermal MEL-TEMP. Single-crystal X-ray crystallography was performed by Dr. Jason Masuda at Saint Mary's University.

#### 2.1.2 Reagents

Anhydrous toluene (99.8%), anhydrous tetrahydrofuran (THF) ( $\geq 99.9\%$ , inhibitor-free), anhydrous diethyl ether ( $\geq 99.7\%$ ), and anhydrous hexane (95%) were obtained from Sigma Aldrich and dried with molecular sieves and sodium metal. Indium (III) chloride anhydrous powder (98%), *n*-butyllithium (1.6M in hexanes), dimethylamine (2.0 M in THF) *N*-bromosuccinimide (NBS), K-Selectride (1.0 M in THF), and 2,2'-azobis(2-methylpropionitrile) (AIBN) were obtained from Sigma Aldrich and used as received. 2-bromo-*m*-xylene, and 1,8-dibromonaphthalene were obtained from TCI America and used as received.

## 2.2 Synthesis of $C_6H_3Br-2,6-(CH_2Br)_2$ (**2**)

### 2.2.1 Synthesis of $C_6H_3Br-2,6-(CH_2Br)_2$ (**2**) Using Ultraviolet Light<sup>28</sup>

A solution of 2-bromo-*m*-xylene (24.93 g, 0.135 mmol), *N*-bromosuccinimide (48.43 g, 0.272 mmol) and AIBN (catalytic amount) in  $CCl_4$  (150 mL) was irradiated with ultraviolet light and refluxed for 3 h. The reaction was then filtered, and the filtrate concentrated via rotary evaporation to give a white slurry. This was then recrystallized by dissolving in hot hexane (150 mL) and cooling to  $-15\text{ }^\circ\text{C}$  to yield colourless needles. Yield: 19.170 g, 55.91 mmol, 41%.  $^1\text{H-NMR}$  ( $CDCl_3$ , ppm): 7.44-7.13 (m, 3H), 4.65 (s, 4H) (Appendix 1).

### 2.2.2 Synthesis of $C_6H_3Br-2,6-(CH_2Br)_2$ (**2**) Using Infrared Light<sup>29</sup>

2-bromo-*m*-xylene (22.206 g, 120.00 mmol) and *N*-bromosuccinimide (46.956 g, 264.00 mmol) were added to methyl acetate (600 mL) to give a white slurry. This solution was irradiated with a 75 W infrared light bulb for 16 h resulting in a clear, pale-yellow solution. The solvent was removed via rotary evaporation and the resulting pale-yellow solid was extracted with boiling hexane (2 x 300 mL) and gravity filtered. Cooling the solution to  $-15\text{ }^\circ\text{C}$  yielded colourless needles. Yield: 27.611 g, 80.53 mmol, 67%.  $^1\text{H-NMR}$  ( $CDCl_3$ , ppm): 7.44-7.20 (m, 3H), 4.65 (s, 4H) (Appendix 2).

## 2.3 Synthesis of $(NCN)Br$ (**3**)<sup>30</sup>

$C_6H_3Br-2,6-(CH_2Br)_2$  (**2**) (10.8 g, 31.5 mmol) and  $Me_2NH$  (2 M in THF, 130 mL, 260 mmol) were added to  $Et_2O$  (300 mL), cooled to  $0\text{ }^\circ\text{C}$  and stirred for 16 h. The solvent was then removed via rotary evaporation to give a yellow-white solid. This solid was then

treated with a 2 M NaOH solution (100 mL) and the product extracted with hexane (2 x 100 mL). The yellow solution was then dried with MgSO<sub>4</sub>, filtered, and concentrated to an orange oil with a rotary evaporator. The product was then flash distilled at 90 °C under vacuum to give a yellow oil. Yield: 6.466 g, 23.84 mmol, 84%. <sup>1</sup>H-NMR (CDCl<sub>3</sub>, ppm): 7.39-7.13 (m, 3H), 3.54 (s, 4H), 2.30 (s, 12H) (Appendix 3).

#### 2.4 Synthesis of (NCN)InCl<sub>2</sub> (4)<sup>31</sup>

Under an atmosphere of dinitrogen, *n*-butyllithium (1.6 M in hexanes, 4.6 mL, 7.37 mmol) was added dropwise to a solution of (NCN)Br (3) (1.997 g, 7.37 mmol) in THF (30 mL) at 23 °C to produce a dark green solution which gradually became orange as it was stirred over 1 h. This solution was then added to a solution of InCl<sub>3</sub> (1.60 g, 7.37 mmol) in THF (30 mL) at 23 °C. This clear amber solution was stirred for 16 h and the solvent removed under reduced pressure to give an orange gel. Toluene (10 mL) was added, the solution was filtered, and the solvent removed under reduced pressure to give a yellow solid. The product was washed with hexane (10 mL) and the hexane removed to give a beige powder. Yield: 1.172 g, 3.108 mmol, 42%. <sup>1</sup>H-NMR (CDCl<sub>3</sub>, ppm): 7.29 (t, J=7.6 Hz, 1H), 7.04 (d, J=7.8 Hz, 1H), 3.60 (s, 4H), 2.51 (s, 12H) (Appendix 4).

#### 2.5 Attempted Synthesis of [(NCN)InCl]<sub>2</sub>(naphth) (5)

Under an atmosphere of dinitrogen, *n*-butyllithium (1.6 M in hexanes, 1.2 mL, 1.98 mmol) was added dropwise to a solution of 1,8-dibromonaphthalene (0.285 g, 0.99 mmol) in THF (20 mL) at -90 °C to give a clear yellow solution. This solution was stirred for 1 h before being added to a solution of (NCN)InCl<sub>2</sub> (4) (0.750 g, 1.98 mmol) in THF (20 mL) at -90 °C. The reaction mixture was allowed to warm to 23 °C over 1 h then heated to reflux

for 16 h resulting in a purple tinged, amber solution. The solvent was then removed under reduced pressure resulting in a yellow-brown gel. This crude product was extracted into toluene (10 mL) and filtered. The filtrate was concentrated to 1 mL and layered with hexane yielding beige powder.

## 2.6 Synthesis of $\text{Li}_2(\text{naphth})(\text{TMEDA})$ (**7**)

Under an atmosphere of dinitrogen, *n*-butyllithium (1.6 M in hexanes, 15 mL, 24.39 mmol) was added dropwise to a solution of 1,8-dibromonaphthalene (3.170 g, 11.09 mmol), and tetramethylethylenediamine (TMEDA) (3.092 g, 26.61 mmol) in hexane (45 mL) at -90 °C resulting in a bright yellow solution. The reaction mixture was allowed to warm slowly over 1.5 h during which it turned cloudy yellow. The solvent was then decanted resulting in a grey solid. This crude product was then washed with hexane (2 x 50 mL) and gravity filtered. The product was dried under vacuum yielding a yellow pyrophoric powder. Yield: 1.526 g, 5.954 mmol, 54 %.  $^1\text{H-NMR}$  (THF- $d_8$ , ppm): 8.09 (d,  $J=4.4$  Hz, 2H), 7.46 (d,  $J=7.0$  Hz, 2H), 7.12 (t,  $J=5.9$  Hz, 2H), 2.32 (s, 4H), 2.14 (s, 12H) (Appendix 5).

## 2.7 Synthesis of $[(\text{NCN})\text{In}]_2(\text{naphth})_2$ (**8**)

Under an atmosphere of dinitrogen, a solution of  $(\text{NCN})\text{InCl}_2$  (**4**) (0.755 g, 1.98 mmol) in THF (10 mL) was added dropwise to a solution of  $\text{Li}_2(\text{naphth})(\text{TMEDA})$  (**7**) (0.2533 g, 0.99 mmol) in THF (10 mL) at -90 °C resulting in an orange solution. The cold bath was removed after 1 h and the reaction mixture stirred for 16 h. The solvent was then removed under reduced pressure resulting in an orange gel. This was extracted into toluene

(2 x 5 mL) and filtered to remove LiCl. The solution was concentrated to 4 mL and placed at -15 °C yielding beige crystals. Yield: 0.167 g, 0.193 mmol, 39%. <sup>1</sup>H-NMR (CDCl<sub>3</sub>, ppm): 7.68-7.56 (m, 8H), 7.27-7.14 (m, 6H), 7.00 (d, J=7.4 Hz, 4H), 3.37 (s, 8H), 1.64 (s, 24H) (Appendix 6). <sup>13</sup>C{<sup>1</sup>H}-NMR (CDCl<sub>3</sub>, ppm): 162.5, 160.6, 148.7, 146.2, 138.3, 134.3, 128.1, 126.4, 125.6, 124.2, 124.1, 66.4, 63.7, 46.4. (Appendix 7). FT-IR (cm<sup>-1</sup>): 3036 m, 2988 w, 2955 w, 2861 m, 2826 s, 2784 m (Appendix 8). FT-Raman (cm<sup>-1</sup>): 3039 vs, 2992 w, 2957 w, 2888 w, 2830 m, 2786 m (Appendix 9). Melting Point: 257.4-258.6 °C.

## 2.8 Attempted Synthesis of [(NCN)InCl]<sub>2</sub> (9)

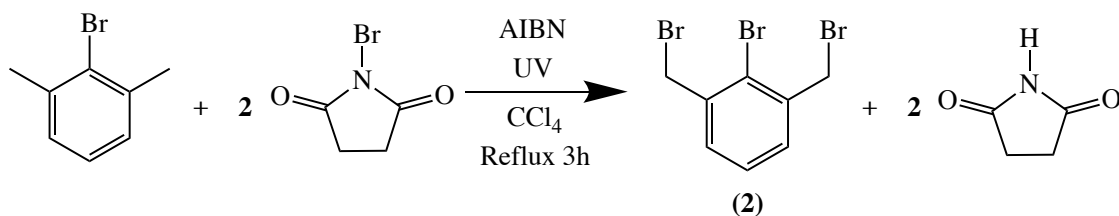
Under an atmosphere of dinitrogen, K-Selectride (1.0 M in THF, 1.2 mL, 1.2 mmol) was added dropwise to a solution of (NCN)InCl<sub>2</sub> (**4**) (0.447 g, 1.17 mmol) in THF (10 mL) at -90 °C to form a yellow solution. The solution was allowed to warm to -10 °C over a period of 3 h before removal of the solvent under reduced pressure resulting in a grey gel. The product was extracted into toluene (10 mL), and the solution filtered to produce a yellow filtrate. The solvent was removed under vacuum and the product dissolved in THF (1 mL), layered with pentane (3 mL) and let sit at 23 °C yielding colourless crystals. Yield: 0.071 g, 0.104 mmol, 18 %. <sup>1</sup>H-NMR (CDCl<sub>3</sub>, ppm): 7.14 (t, J=9.8, 2H), 7.00 (d, J=7.6, 4H), 3.59-3.49 (m, 8H), 2.48 (s, 24H) (Appendix 10).

### 3. Results and Discussion

#### 3.1 Synthesis of $C_6H_3Br-2,6-(CH_2Br)_2$ (**2**)

##### 3.1.1 Synthesis of $C_6H_3Br-2,6-(CH_2Br)_2$ (**2**) Using Ultraviolet Light

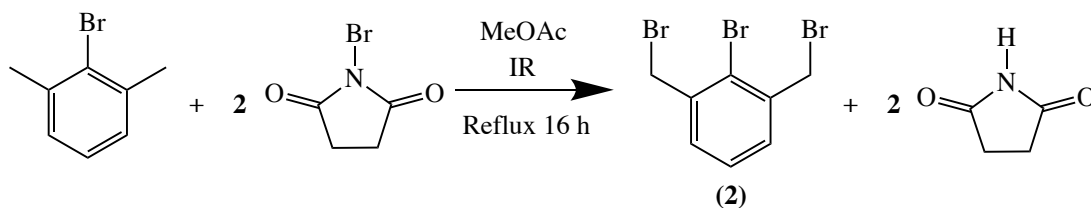
Initial attempts to synthesis  $C_6H_3Br-2,6-(CH_2Br)_2$  (**2**) were adapted from a literature procedure in which 2-bromo-*m*-xylene, NBS, and AIBN are refluxed in  $CCl_4$ .<sup>28</sup> This reaction in the absence of UV light and radical initiator did not yield the desired product. It was found that UV light was necessary to initiate the free radical bromination (Scheme 1).<sup>30</sup> This adapted synthesis resulted in poor yields (26-41%) and incomplete reaction of the starting material. The hexane extraction resulted in colourless needles of **2** when cooled, with the unreacted 2-bromo-*m*-xylene remaining in solution. Attempts to reuse recovered 2-bromo-*m*-xylene resulted in a mixture of the intended tribromide product **2** and the pentabromide  $C_6H_3Br-2,6-(CHBr_2)_2$ . In the  $^1H$ -NMR spectrum of  $C_6H_3Br-2,6-(CHBr_2)_2$  the  $C_6H_3$  signal appears as a doublet at 8.04 ppm. When crystalized from hexane solution **2** appears as colourless needles while  $C_6H_3Br-2,6-(CHBr_2)_2$  appears as a clumped white solid. Attempts to separate these products using column chromatography were unsuccessful. Initial attempts at this synthesis used old samples of NBS which was coloured yellow, and AIBN. Attempting the reaction with newly purchased NBS which was coloured white, and AIBN resulted in increased yields (41-47%).



**Scheme 1:** Synthesis of  $C_6H_3Br-2,6-(CH_2Br)_2$  (**2**) from 2-bromo-*m*-xylene and NBS using ultraviolet light and AIBN to initiate radical reaction.

### 3.1.2 Synthesis of $C_6H_3Br-2,6-(CH_2Br)_2$ (**2**) Using Infrared Light

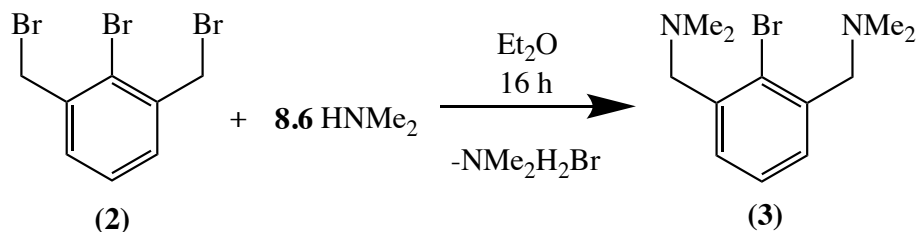
To eliminate the need for the expensive and the environmentally harmful solvent  $CCl_4$ , an alternative synthetic method for **2** was found which eliminates the need for chlorinated solvent (Scheme 2).<sup>29</sup> This procedure uses a 75 W infrared bulb which, along with wrapping the round bottom flask with aluminum foil, provides the heat to bring the solution to reflux. The solution of NBS and 2-bromo-*m*-xylene appears as a white slurry which becomes a clear pale-yellow solution after the 16 h stir. Removal of the solvent results in a dull yellow powder which can then be extracted into boiling hexane and gravity filtered. The product readily crystallizes when cooled to give colourless needles. The product was collected after 24 h to give a 67% yield. Further cooling of the reaction solution yields a small amount of light pink solid. The  $^1H$ -NMR spectrum of this material shows that it is a mixture of **2** and  $C_6H_3Br-2,6-(CHBr_2)_2$ , again showing that the reaction produces small amounts of pentabromide as a side product.



**Scheme 2:** Synthesis of  $C_6H_3Br-2,6-(CH_2Br)_2$  (**2**) from 2-bromo-*m*-xylene and NBS using infrared light.

### 3.2 Synthesis of (NCN)Br (**3**)

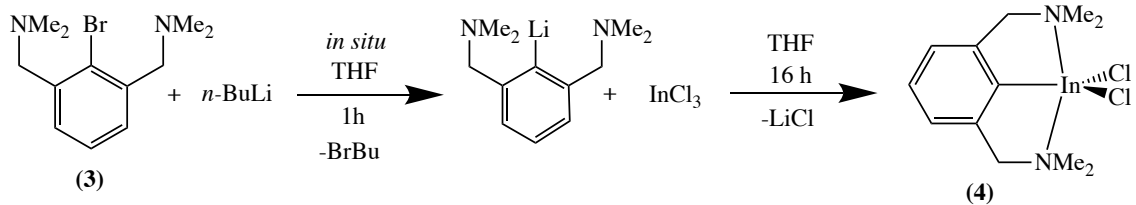
(NCN)Br (**3**) can be synthesized from the reaction of dimethyl amine and **2** in diethyl ether (Scheme 3).<sup>30</sup> The reaction mixture is cloudy white and forms a white precipitate as the reaction proceeds. Removal of the solvent results in white-yellow solid which is then treated with NaOH solution and extracted into hexane. This yellow solution is then dried with  $MgSO_4$  and concentrated down to an orange oil. The product is then distilled under vacuum at  $90\text{ }^\circ\text{C}$  to give a yellow or orange oil. The literature procedure reports the product as a colourless oil which could indicate that there are bromine impurities present in the distilled product.<sup>30</sup> A second distillation would likely remove these impurities. Yields are good for this reaction (55-86%) and increase as the reaction is scaled up.



**Scheme 3:** Amination of  $C_6H_3Br-2,6-(CH_2Br)_2$  (**2**) to synthesize (NCN)Br (**3**).

### 3.3 Synthesis of (NCN)InCl<sub>2</sub> (4)

It is reported that (NCN)InCl<sub>2</sub> (4) can be synthesized from 3 and InCl<sub>3</sub> in hexane.<sup>31</sup> It was found that both the starting material and product do not dissolve into hexane or diethyl ether and instead form suspensions. Therefore, the synthesis was attempted in hexane, THF and toluene with identical reaction condition to determine the ideal solvent. Yields were 34% for hexane, 38% for THF, and 42% for toluene. It was determined that THF was the best choice of solvent as it can dissolve both the starting material and the product (Scheme 4). After stirring for 16 h the solvent was removed under vacuum to give the crude product as an orange gel. The original literature procedure for this reaction calls for the product to be sublimed from the crude material.<sup>31</sup> It was found that though sublimation produces pure product, it is time intensive and produces yields too low to be a viable source of starting material (8-9%). It was determined that an extraction of the product from the crude material was necessary. The product was extracted into toluene and filtered to remove LiCl produced by the reaction. The solvent was then removed to produce a clumpy orange solid. Washing this solid with hexane followed by removal of the hexane under vacuum produces fine beige powder. Yields for this reaction in THF with toluene extraction are 30-59% with yields again increasing as the reaction is scaled up.



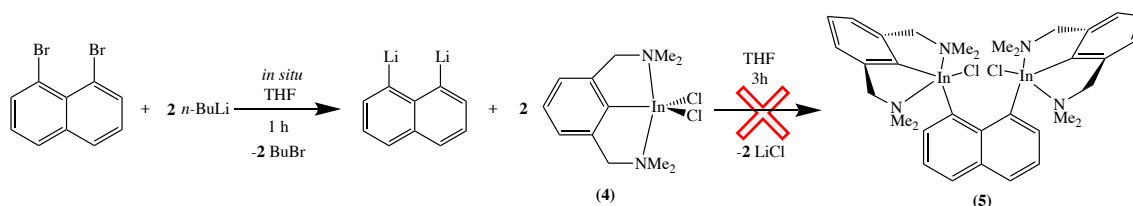
**Scheme 4:** *In situ* generation of (NCN)Li from (NCN)Br (**3**) and *n*-butyllithium and subsequent reaction with InCl<sub>3</sub> to form (NCN)InCl<sub>2</sub> (**4**).

### 3.4 Attempted Synthesis of [(NCN)InCl]<sub>2</sub>(naphth) (**5**)

Initial attempts to synthesize [(NCN)InCl]<sub>2</sub>(naphth) (**5**) involved generating Li<sub>2</sub>(naphth) *in situ* by reacting 1,8-dibromonaphthalene with two equivalents of *n*-butyllithium at 23 °C followed by reaction with (NCN)InCl<sub>2</sub> (**4**). Again, it was found that THF was the preferred solvent for this reaction as the products and starting materials are insoluble in hexane and diethyl ether and instead form suspensions. Initial trials had a theoretical yield of 400 mg of **5** and attempts to crystallize the product out of a solution of toluene, and toluene with hexane layering were unsuccessful. When the reaction yield was doubled to 800 mg, layering a 1 mL toluene solution with hexane saw formation of beige crystals. These crystals were determined to be (NCN)InBr<sub>2</sub> (**6**) by X-ray crystallography (Section 3.8).

It was theorized that the 1-bromobutane generated by the reaction of 1,8-dibromonaphthalene with *n*-butyllithium was reacting with the (NCN)InCl<sub>2</sub> generating (NCN)InBr<sub>2</sub>. To solve this problem, both the initial addition of *n*-butyllithium to 1,8-dibromonaphthalene and the addition of Li<sub>2</sub>(naphth) to **4** were carried out at -90 °C. This was followed by heating the reaction mixture at reflux to give the reactants sufficient

energy to form **5**. Attempts to crystallize the resulting product from toluene, toluene with hexane layering, and DCM were unsuccessful. Removal of the solvent gave a beige powder and a brown gel suggesting that there were multiple products.  $^1\text{H-NMR}$  data does not show evidence of the naphth ligand with only the NCN peaks appearing. It was determined that it is necessary to isolate  $\text{Li}_2(\text{naphth})$  rather than generating it *in situ*.

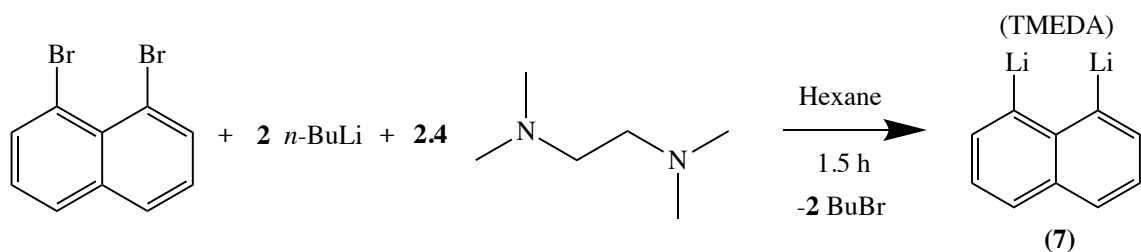


**Scheme 5:** Attempted synthesis of  $[(\text{NCN})\text{InCl}_2](\text{naphth})$  (**5**). Attempts to generate  $\text{Li}_2(\text{naphth})$  *in situ* and subsequently react it with  $(\text{NCN})\text{InCl}_2$  (**4**) were unsuccessful and instead resulted in generation of  $(\text{NCN})\text{InBr}_2$  (**6**).

### 3.5 Synthesis of $\text{Li}_2(\text{naphth})(\text{TMEDA})$ (**7**)

$\text{Li}_2(\text{naphth})(\text{TMEDA})$  was synthesized from the reaction of 1,8-dibromonaphthalene and *n*-butyllithium in the presence of excess TMEDA (Scheme 6). This procedure was adapted from the conditions outlined by K. M. Rabanzo-Castillo *et al.*, which describes the *in situ* preparation of  $\text{Li}_2(\text{naphth})$  from 1,8-dibromonaphthalene and *n*-butyllithium and T. Shimamura *et al.*, which describes the production of  $\text{Li}(\text{naphth})(\text{TMEDA})$  from 1-bromonaphthalene and *n*-butyllithium in the presence of excess TMEDA and  $\text{Li}_2(\text{naphth})(\text{TMEDA})$  from  $\text{Li}(\text{naphth})(\text{TMEDA})$  and *n*-butyllithium in the presence of excess TMEDA.<sup>32,33</sup> A slight excess of TMEDA is used per molecule of *n*-butyllithium added, though  $^1\text{H-NMR}$  data suggests that only a single molecule of

TMEDA is associated with each molecule of **7**. The ethanol cold bath used was cooled to  $-90\text{ }^{\circ}\text{C}$  which rises to  $-30\text{ }^{\circ}\text{C}$  after the reaction mixture stirs for 1.5 h. The solvent was then removed under vacuum and the product was washed with hexane. The wash is coloured, which lessens with each successive wash. The product was then dried under vacuum. The resulting yellow powder readily ignites when exposed to air. When stored in an uncovered flask the material touching the sides of the vessel turn purple indicating that the compound is light sensitive. When stored in a vial wrapped in aluminum foil the yellow colour does not degrade with time.

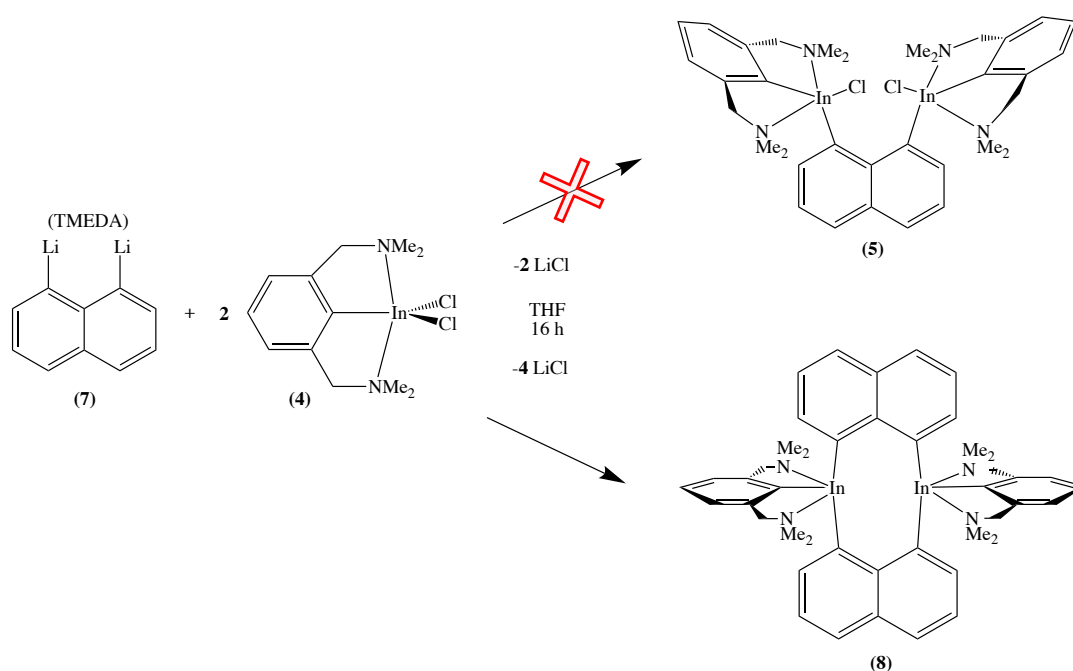


**Scheme 6:** Synthesis of Li<sub>2</sub>(naphth)(TMEDA) (**7**) from 1,8-dibromonaphthalene, *n*-butyllithium, and TMEDA. Though an excess of TMEDA is used per molecule of *n*-butyllithium added, <sup>1</sup>H-NMR shows that only a single TMEDA is bound per molecule of **7**.

### 3.6 Synthesis of [(NCN)In]<sub>2</sub>(naphth)<sub>2</sub> (**8**)

Li<sub>2</sub>(naphth)(TMEDA) (**7**) was reacted with (NCN)InCl<sub>2</sub> (**4**) in 1:2 ratio in THF at  $-90\text{ }^{\circ}\text{C}$  in an attempt to synthesize [(NCN)InCl]<sub>2</sub>(naphth) (**5**) (Scheme 7). The solvent was removed under vacuum and the product dissolved in toluene to allow separation of the LiCl by-product. The product was then crystallized by concentrating and cooling the resulting solution. The <sup>1</sup>H-NMR spectrum of the crystalline product indicated that **5** was successfully

made. X-ray crystallography data showed that the crystalline material was  $[(\text{NCN})\text{In}]_2(\text{naphth})_2$  (**8**) (Section 3.8) indicating that the steric bulk of the NCN ligand is not sufficient to prevent multiple 1,8-naphthalide molecules from reacting with **4**. This structure is similar to what was observed by Hoefelmeyer *et al.* for the reaction of  $\text{InCl}_3$  with **7** in the presence of pyridine to produce  $[\text{InCl}(\text{pyr})_2]_2(\text{naphth})_2$  (Figure 13).<sup>34</sup> Yields are low for the synthesis of **8** as **7** was reacted with two equivalents of **4** to yield a 1:1 product. This leads to naphthalene being a limiting reagent and unreacted excess **4** staying in solution and appearing in  $^1\text{H-NMR}$  spectrum (Appendix 6).



**Scheme 7:** Synthesis of  $[(\text{NCN})\text{In}]_2(\text{naphth})_2$  (**8**) from  $\text{Li}_2(\text{naphth})(\text{TMEDA})$  (**7**) and  $(\text{NCN})\text{InCl}_2$  (**4**).

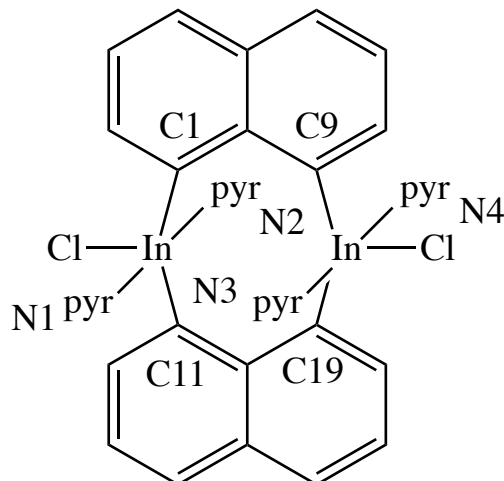
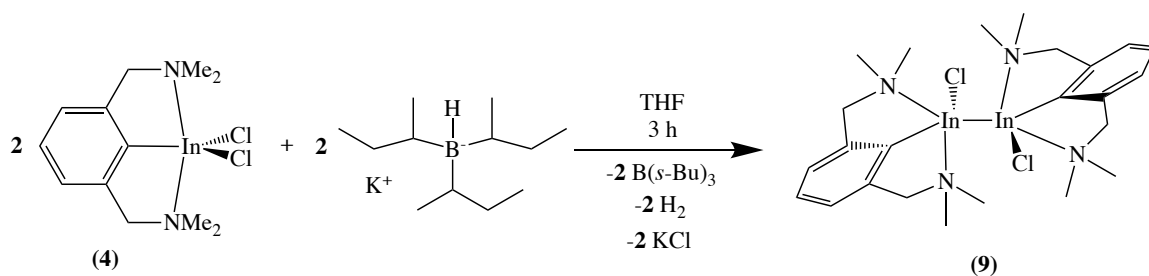


**Figure 13:** The structure of  $[\text{InCl}(\text{pyr})_2]_2(\text{naphth})_2$  as observed by Hoefelmeyer *et al.*

### 3.7 Attempted Synthesis of $[(\text{NCN})\text{InCl}]_2$ (**9**)

As intermediate **5** could not be prepared, an alternative synthetic route was devised which involves the synthesis of the diindane  $[(\text{NCN})\text{InCl}]_2$  (**9**) followed by reaction with **7**. Experimental details for the synthesis of **9** are based on those described by Lomeli *et al.*<sup>23</sup> K-Selectride (potassium tri(*sec*-butyl)borohydride) is chosen as a reducing agent as it has been shown to reduce bismuth compounds with similar polydentate ligands.<sup>35</sup> Addition of K-Selectride to a clear solution of **4** in THF at  $-90\text{ }^\circ\text{C}$  (Scheme 8) yields a cloudy yellow solution, suggesting formation of KCl. Initial attempts at this reaction involved removal of the cold bath 10 min after addition of K-Selectride. The yellow solution rapidly turns to an opaque grey upon warming which suggests reduction of **4** to elemental indium. Removal of the solvent under vacuum followed by extraction into toluene and filtration removes this grey solid from the solution leaving yellow filtrate. Removal of toluene from the filtrate produced a thick green-grey solution. The  $^1\text{H-NMR}$  spectrum of the green-grey solution shows large amount of tri-*sec*-butyl borane and small amounts of the NCN ligand.

This reaction was attempted a second time with the solution left to stir over cold bath to prevent reduction of indium. After 3 h the bath temperature had risen to  $-10\text{ }^{\circ}\text{C}$  and the solution began to turn an opaque green-grey. The solvent was removed under vacuum to give a grey gel. This was extracted into toluene and filtered to remove grey solid from a yellow filtrate. Removal of toluene produced a small amount of white solid in a yellow solution. The  $^1\text{H-NMR}$  spectrum of the product again shows large amount of tri-*sec*-butyl borane produced from K-Selectride and small amounts of the NCN ligand suggesting that this remaining solution is liquid tri-*sec*-butyl borane. When this solution was dissolved in 1 mL of THF and layered with pentane colourless crystals were produced at  $23\text{ }^{\circ}\text{C}$ . The  $^1\text{H-NMR}$  spectrum of the product (Appendix 10) shows that the aryl and methyl peaks shift relative to the  $^1\text{H-NMR}$  spectrum of **4** (Appendix 4). The  $\text{C}_6\text{H}_3\text{CH}_2$  peak of the NCN ligand now appear as a multiplet rather than a singlet, suggesting that the bonds are now locked in place resulting in inequivalence between the two hydrogen atoms. This evidence suggests that **9** was made successfully.



**Scheme 8:** Synthesis of  $[(\text{NCN})\text{InCl}]_2$  (**9**) from  $(\text{NCN})\text{InCl}_2$  (**4**) using K-Selectride as a reducing agent.

### 3.8 X-Ray Crystal Structures

The X-ray crystal structures of  $(\text{NCN})\text{InBr}_2$  (**6**) and  $[(\text{NCN})\text{In}]_2(\text{naphth})_2$  (**8**) are shown in Figure 14 and Figure 15, respectively. The preliminary structure of **6** features

indium in a distorted trigonal bipyramidal bonding arrangement with equatorial bonds to the C1 of the NCN ligand and two bromine atoms, with the coordinating nitrogen atoms from the NCN ligand occupying axial positions.

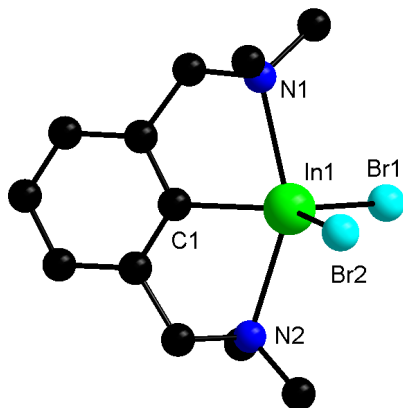


**Figure 14:** X-ray crystal structure of (NCN)InBr<sub>2</sub> (**6**).

The solid-state structure of **8** shows In in a distorted trigonal bipyramidal bonding arrangement. Each indium atom is bonded to C1 of the NCN ligand as well as two naphth ligands. The nitrogen atoms of the NCN amine groups again occupy the axial positions.

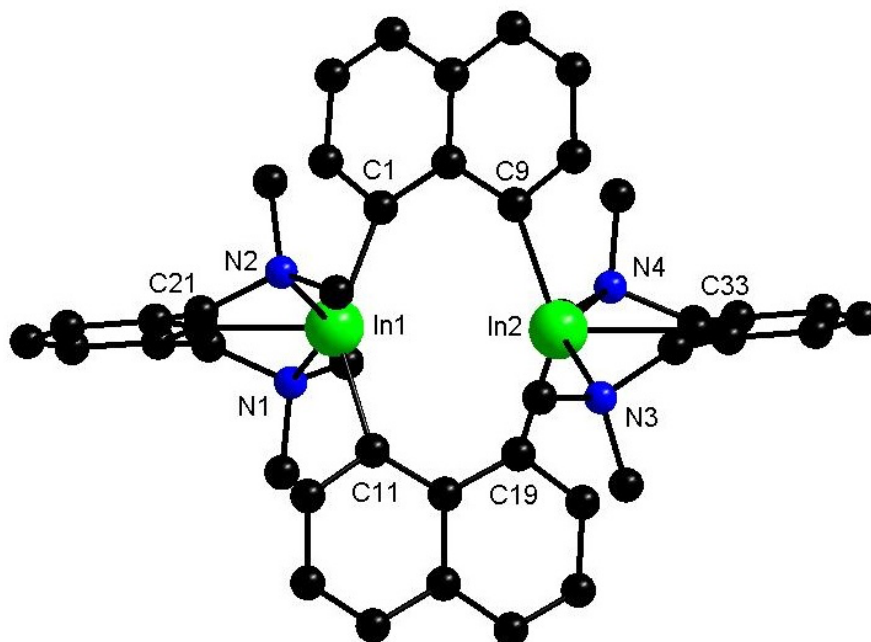


**Figure 15:** X-ray crystal structure of  $[(\text{NCN})\text{In}]_2(\text{naphth})_2$  (**8**). Selected bond distances ( $\text{\AA}$ ) and angles ( $^\circ$ ):  $\text{In1-C1} = 2.150(9)$ ,  $\text{In1-C11} = 2.170(8)$ ,  $\text{In1-C21} = 2.165(8)$ ,  $\text{In1-N1} = 2.610(8)$ ,  $\text{In1-N2} = 2.568(8)$ ,  $\text{In2-C9} = 2.181(9)$ ,  $\text{In2-C19} = 2.181(9)$ ,  $\text{In2-C33} = 2.21(6)$ ,  $\text{In2-N3} = 2.63(6)$ ,  $\text{In2-N4} = 2.49(2)$ ,  $\text{C1-In1-C11} = 143.4(3)$ ,  $\text{C1-In1-C21} = 109.6(3)$ ,  $\text{C11-In1-C21} = 107.0(3)$ ,  $\text{N1-In1-N2} = 144.8(3)$ ,  $\text{C9-In2-C19} = 143.8(3)$ ,  $\text{C9-In2-C33} = 108.0(8)$ ,  $\text{C19-In2-C33} = 108.2(8)$ ,  $\text{N3-In1-N4} = 141.4(5)$

As previously mentioned, the solid-state structure of **8** is similar to what is seen in  $[\text{InCl}(\text{pyr})_2]_2(\text{naphth})_2$  as synthesized by Hoefelmeyer *et al.* (Figure 13).<sup>34</sup> In  $[\text{InCl}(\text{pyr})_2]_2(\text{naphth})_2$  indium is a distorted trigonal bipyramidal structure with equatorial bonds to a chlorine atom and two naphthalide ligands. Axial positions are occupied by nitrogen atoms from pyridine. Table 1 compares the bond lengths of these compounds and Table 2 the bond angles.

**Table 1:** Comparisons of bond distances (Å) of **8** and [InCl(pyr)<sub>2</sub>]<sub>2</sub>(naphth)<sub>2</sub>.<sup>34</sup>

	<b>8</b>	[InCl(pyr) <sub>2</sub> ] <sub>2</sub> (naphth) <sub>2</sub>
In1-C1	2.150(9)	2.163(3)
In1-C11	2.170(8)	2.174(3)
In1-N1	2.610(8)	2.524(2)
In1-N2	2.568(8)	2.468(2)

**Table 2:** Comparisons of bond angles (°) of **8** and [InCl(pyr)<sub>2</sub>]<sub>2</sub>(naphth)<sub>2</sub>.<sup>34</sup>

	<b>8</b>	[InCl(pyr) <sub>2</sub> ] <sub>2</sub> (naphth) <sub>2</sub>
C1-In1-C11	143.4(3)	153.3(1)
N1-In1-N2	144.8(3)	163.48(7)

## 4. Conclusion

Reliable synthetic procedures were developed for the synthesis of C<sub>6</sub>H<sub>3</sub>Br-2,6-(CH<sub>2</sub>Br)<sub>2</sub> (**2**), (NCN)Br (**3**), (NCN)InCl<sub>2</sub> (**4**), Li<sub>2</sub>(naphth)(TMEDA) (**7**), and [(NCN)In]<sub>2</sub>(naphth)<sub>2</sub> (**8**) and these products were fully characterized. It was determined that it was necessary to isolate **7** for further reaction rather than generating it *in situ*. Attempts to produce [(NCN)InCl]<sub>2</sub>(naphth) (**5**) instead generated [(NCN)In]<sub>2</sub>(naphth)<sub>2</sub> (**8**), indicating that the steric bulk of the NCN ligand is insufficient to prevent reaction with

multiple naphthalide ligands. An alternate synthetic route to the target diindane is therefore required. This alternate synthetic route sees synthesis of the diindane  $[(\text{NCN})\text{InCl}]_2$  (**9**) followed by reaction with **7** to generate the target diindane  $[(\text{NCN})_2\text{In}_2(\text{naphth})]$  (**1**). Preliminary evidence suggests **4** may be reduced to **9** using K-Selectride.

## 5. Future Directions

In the future  $(\text{NCN})\text{InCl}_2$  (**4**) and  $\text{Li}_2(\text{naphth})(\text{TMEDA})$  (**7**) will be reacted in a 1:1 ratio to develop an improved procedure for the synthesis of the novel compound  $[(\text{NCN})\text{In}]_2(\text{naphth})_2$  (**8**). The pure product will then be characterized using elemental analysis. A reliable synthetic procedure for  $[(\text{NCN})\text{InCl}]_2$  (**9**) must be developed that prevents reduction of **4** to elemental indium. Once this compound is isolated and characterized it must be reacted with **7** to yield the target diindane  $[(\text{NCN})_2\text{In}_2(\text{naphth})]$  (**1**). A synthetic work up for **1** must be developed which produces crystals suitable for structural analysis using single crystal X-ray crystallography. **1** will then be fully characterized and tested for redox activity using cyclic voltammetry and for reactivity with disulfides.

## 6. References

- (1) Anastas, P.; Eghbali, N. Green Chemistry: Principles and Practice. *Chemical Society Reviews*. **2010**, *39*, 301–312.
- (2) Poliakoff, M. Green Chemistry: Science and Politics of Change. *Science*. **2002**, *297*, 807–810.
- (3) Sheldon, R. A. The E Factor 25 Years on: The Rise of Green Chemistry and Sustainability. *Green Chemistry*. **2017**, *19*, 18–43.
- (4) Dunn, P. J.; Galvin, S.; Hettenbach, K. The Development of an Environmentally Benign Synthesis of Sildenafil Citrate (Viagra<sup>TM</sup>) and Its Assessment by Green Chemistry Metrics. *Green Chemistry*. **2004**, *6*, 43–48.
- (5) Cue, B. W.; Zhang, J. Green Process Chemistry in the Pharmaceutical Industry. *Green Chemistry Letters and Reviews*. **2009**, *2*, 193–211.
- (6) Alfonsi, K.; Colberg, J.; Dunn, P. J.; Fevig, T.; Jennings, S.; Johnson, T. A.; Kleine, H. P.; Knight, C.; Nagy, M. A.; Perry, D. A.; Stefaniak, M. Green Chemistry Tools to Influence a Medicinal Chemistry and Research Chemistry Based Organisation. *Green Chemistry*. **2008**, *10*, 31–36.
- (7) Anastas, P. T.; Kirchhoff, M. M.; Williamson, T. C. Catalysis as a Foundational Pillar of Green Chemistry. *Applied Catalysis A: General*. **2001**, *221*, 3–13.
- (8) Presidential Green Chemistry Challenge Awards Program: Summary of 1997 Award Entries and Recipients. 2.
- (9) Egorova, K. S.; Ananikov, V. P. Which Metals Are Green for Catalysis? Comparison of the Toxicities of Ni, Cu, Fe, Pd, Pt, Rh, and Au Salts. *Angewandte Chemie International Edition*. **2016**, *55*, 12150–12162.

- (10) Ludwig, J. R.; Schindler, C. S. Catalyst: Sustainable Catalysis. *Chem.* **2017**, *2*, 313–316.
- (11) Duckett, S. B.; Newell, C. L.; Eisenberg, R. Observation of New Intermediates in Hydrogenation Catalyzed by Wilkinson's Catalyst,  $\text{RhCl}(\text{PPh}_3)_3$ , Using Parahydrogen-Induced Polarization. *Journal of the American Chemical Society.* **1994**, *116*, 10548–10556.
- (12) Michrowska, A.; Gułajski, Ł.; Kaczmarska, Z.; Mennecke, K.; Kirschning, A.; Grela, K. A Green Catalyst for Green Chemistry: Synthesis and Application of an Olefin Metathesis Catalyst Bearing a Quaternary Ammonium Group. *Green Chemistry.* **2006**, *8*, 685–688.
- (13) Smichowski, P.; Gómez, D.; Frazzoli, C.; Caroli, S. Traffic-Related Elements in Airborne Particulate Matter. *Applied Spectroscopy Reviews.* **2007**, *43*, 23–49.
- (14) Schneider, U.; Kobayashi, S. Low-Oxidation State Indium-Catalyzed C–C Bond Formation. *Accounts of Chemical Research.* **2012**, *45*, 1331–1344.
- (15) Capello, C.; Fischer, U.; Hungerbühler, K. What Is a Green Solvent? A Comprehensive Framework for the Environmental Assessment of Solvents. *Green Chemistry.* **2007**, *9*, 927.
- (16) Dagorne, S.; Fliedel, C.; de Frémont, P. Gallium and Indium Compounds in Homogeneous Catalysis. In *Encyclopedia of Inorganic and Bioinorganic Chemistry*; Scott, R. A., Ed.; John Wiley & Sons, Ltd: Chichester, UK, 2016; pp 1–27.
- (17) Briand, G. G.; Cairns, S. A.; Decken, A.; Dickie, C. M.; Kostelnik, T. I.; Shaver, M. P. Strained Metal Bonding Environments in Methylindium Dithiolates and Their

- Reactivity as Initiators for the Ring-Opening Polymerization of Cyclic Esters. *Journal of Organometallic Chemistry*. **2016**, *806*, 22–32.
- (18) Osten, K. M.; Mehrkhodavandi, P. Indium Catalysts for Ring Opening Polymerization: Exploring the Importance of Catalyst Aggregation. *Accounts of Chemical Research*. **2017**, *50*, 2861–2869.
- (19) Shen, Z.-L.; Wang, S.-Y.; Chok, Y.-K.; Xu, Y.-H.; Loh, T.-P. Organoindium Reagents: The Preparation and Application in Organic Synthesis. *Chemical Reviews*. **2013**, *113*, 271–401.
- (20) Pardoe, J. A. J.; Downs, A. J. Development of the Chemistry of Indium in Formal Oxidation States Lower than +3. *Chemical Reviews*. **2007**, *107*, 2-45.
- (21) Tuck, D. G. The Lower Oxidation States of Indium. *Chemical Society Reviews*. **1993**, *22*, 269-276.
- (22) Haaland, A.; Martinsen, K.-G.; Volden, H. V.; Kaim, W.; Waldhör, E.; Uhl, W.; Schütz, U. Gas-Phase Structure of the Monomeric Alkylgallium(I) Compound  $\text{Ga}[\text{C}(\text{SiMe}_3)_3]$  and the Electrochemical Behavior of  $\text{Ga}_4[\text{C}(\text{SiMe}_3)_3]_4$  and  $\text{In}_4[\text{C}(\text{SiMe}_3)_3]_4$  with EPR Evidence for a  $\text{Ga}_4\text{R}_4$  Radical Anion. *Organometallics*. **1996**, *15*, 1146–1150.
- (23) Lomelí, V.; McBurnett, B. G.; Cowley, A. H. An Indium(II)-Indium(II) Compound with Intramolecular Donor-Acceptor Bonds. *Journal of Organometallic Chemistry*. **1998**, *562*, 123–125.
- (24) Veith, M.; Goffing, F.; Becker, S.; Huch, V. Spezielle Silazanderivate von Digallan(4) und Diindan(4) mit Ga-Ga- bzw. In-In-Bindung. *Journal of Organometallic Chemistry*. **1991**, *406*, 105-118.

- (25) Fryzuk, M. D.; Giesbrecht, G. R.; Rettig, S. J.; Yap, G. P. A. Synthesis and Characterization of Group 13 Hydrides and Metal-Metal Bonded Dimers Stabilized by the Macrocyclic Bis(Amidophosphine) Ligand  $[P_2N_2]$  ( $[P_2N_2]=[PhP(CH_2SiMe_2NSiMe_2CH_2)_2PPh]$ ). *Journal of Organometallic Chemistry*. **1999**, *591*, 63–70.
- (26) Uhl, W.; Hannemann, F.; Wartchow, R. Reactions of Tetraalkyldiindane(4),  $R_2In-InR_2$  ( $R=CH(SiMe_3)_2$ ), with *tert*-Butyl and Phenyl Isonitriles. Formation of Adducts with Retention of the In–In Bond  $\dagger$ . *Organometallics*. **1998**, *17*, 3822–3825.
- (27) Uhl, W.; Graupner, R. The Insertion of Chalcogen Atoms into the In–In Bond of Tetrakis[Bis(Trimethylsilyl)methyl]Diindane(4): Monomeric Compounds with In–S–In, In–Se–In, and In–Te–In Groups. *Journal of Organometallic Chemistry*. **1996**, *523*, 227–234.
- (28) Bibal, C.; Mazières, S.; Gornitzka, H.; Couret, C. New Arylchlorogermynes Stabilized by Two Ortho Side-Chain Donor Ligands. *Polyhedron*. **2002**, *21*, 2827–2834.
- (29) Amijs, C. H. M.; van Klink, G. P. M.; van Koten, G. Carbon Tetrachloride Free Benzylic Brominations of Methyl Aryl Halides. *Green Chemistry*. **2003**, *5*, 470.
- (30) Steenwinkel, P.; James, S. L.; Gossage, R. A.; Grove, D. M.; Kooijman, H.; Smeets, W. J. J.; Spek, A. L.; van Koten, G. Sequential C–H and C–Ru Bond Formation and Cleavage during the Thermally Induced Rearrangement of Aryl Ruthenium(II) Complexes with  $[C_6H_3(CH_2NMe_2)_2-2,6]^-$  as a Bidentate  $\eta^2-C,N$  Coordinated Ligand. The Crystal Structures of the Isomeric Pairs  $[RuCl\{\eta^6-C_{10}H_{14}\}\{\eta^2-C,N-$

- $C_6H_3(CH_2NMe_2)_{2-2,n}$ ] ( $n = 4$  or  $6$ ) and  $[Ru(\eta^5-C_5H_5)\{\eta^2-C,N-C_6H_3(CH_2NMe_2)_{2-2,n}\}(PPh_3)]$  ( $n = 4$  or  $6$ ). *Organometallics*. **1998**, *17*, 4680-4693.
- (31) Schumann, H.; Wassemumn, W.; Dietrich, A. Synthesis and Molecular Structure of  $CH_3\{2,6-[(C_2H_5)_2NCH_2]_2C_6H_3\}InCl$ , an Intramolecular Stabilized Monomeric Diorganoinidium Chloride. *Journal of Organometallic Chemistry*. **1989**, *365*, 11-18.
- (32) Rabanzo-Castillo, K.M.; Hanif, M.; Söhnel, T.; Leitao, E.M. Synthesis, characterization and electronic properties of naphthalene bridged disilanes. *Dalton Transactions*. **2019**, *48*, 13971-13980.
- (33) Shimamura, T.; Maeno, Y.; Kubo, K.; Kume, S.; Greco, C.; Mizuta, T. Protonation and Electrochemical Properties of a Bisphosphide Diiron Hexacarbonyl Complex Bearing Amino Groups on the Phosphide Bridge. *Dalton Transactions*. **2019**, *48*, 16595–16603.
- (34) Hoefelmeyer, J. D.; Schulte, M.; Gabbai, F. P. Synthesis of a Diindacycle by Transmetalation of 1,8-Bis(Trimethylstannyl)Naphthalene with  $InCl_3$ . *Inorganic Chemistry*. **2001**, *40*, 3833–3834.
- (35) Vránová, I.; Alonso, M.; Lo, R.; Sedlák, R.; Jambor, R.; Růžička, A.; Proft, F. D.; Hobza, P.; Dostál, L. From Dibismuthenes to Three- and Two-Coordinated Bismuthinidenes by Fine Ligand Tuning: Evidence for Aromatic  $BiC_3N$  Rings through a Combined Experimental and Theoretical Study. *Chemistry a European Journal*. **2015**, *21*, 16917–16928.

## 7. Appendix

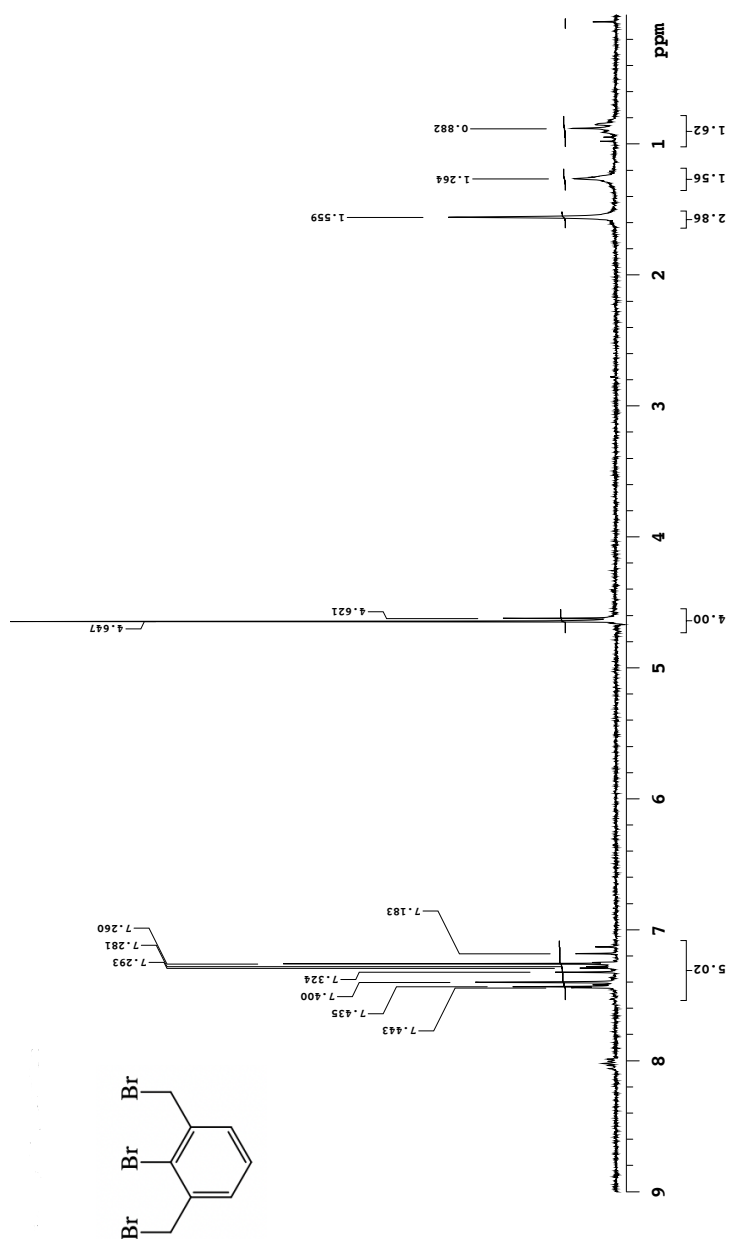


**Figure A.1:**  $^1\text{H-NMR}$  spectrum in  $\text{CDCl}_3$  of  $\text{C}_6\text{H}_3\text{Br}-2,6-(\text{CH}_2\text{Br})_2$  (2) produced from reaction with ultraviolet light.

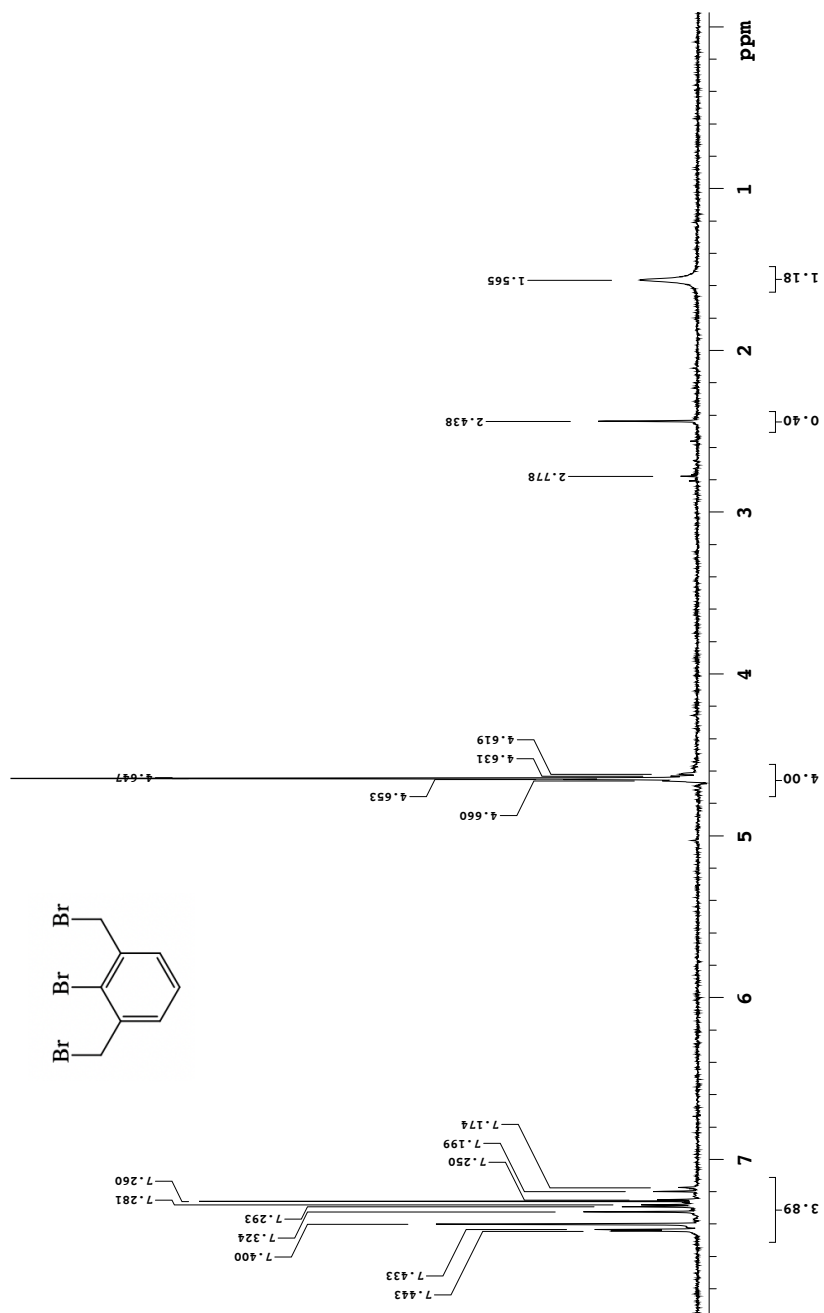


**Figure A.2:**  $^1\text{H-NMR}$  spectrum in  $\text{CDCl}_3$  of  $\text{C}_6\text{H}_3\text{Br}-2,6-(\text{CH}_2\text{Br})_2$  (**2**) from reaction with infrared light.

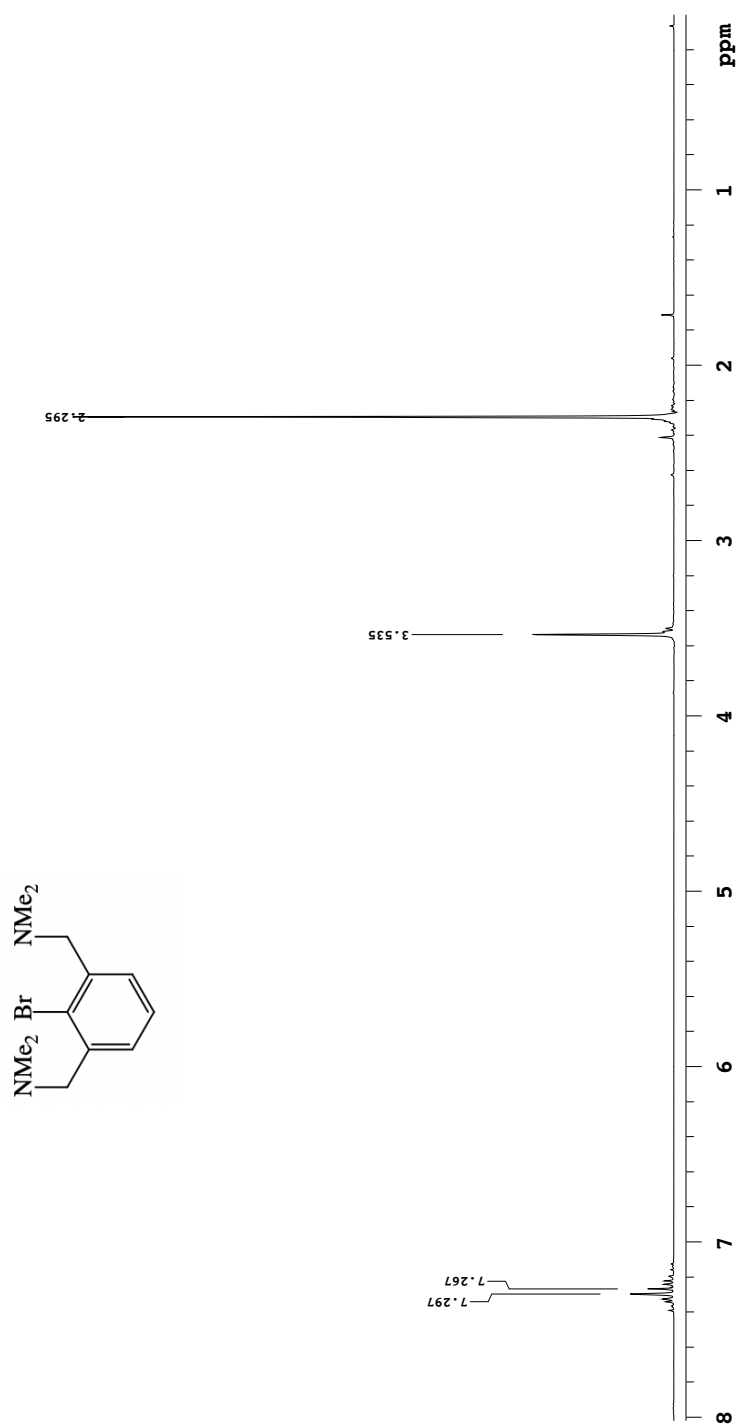


**Figure A.3:**  $^1\text{H-NMR}$  spectrum of (NCN)Br (**3**) in CDCl<sub>3</sub>.

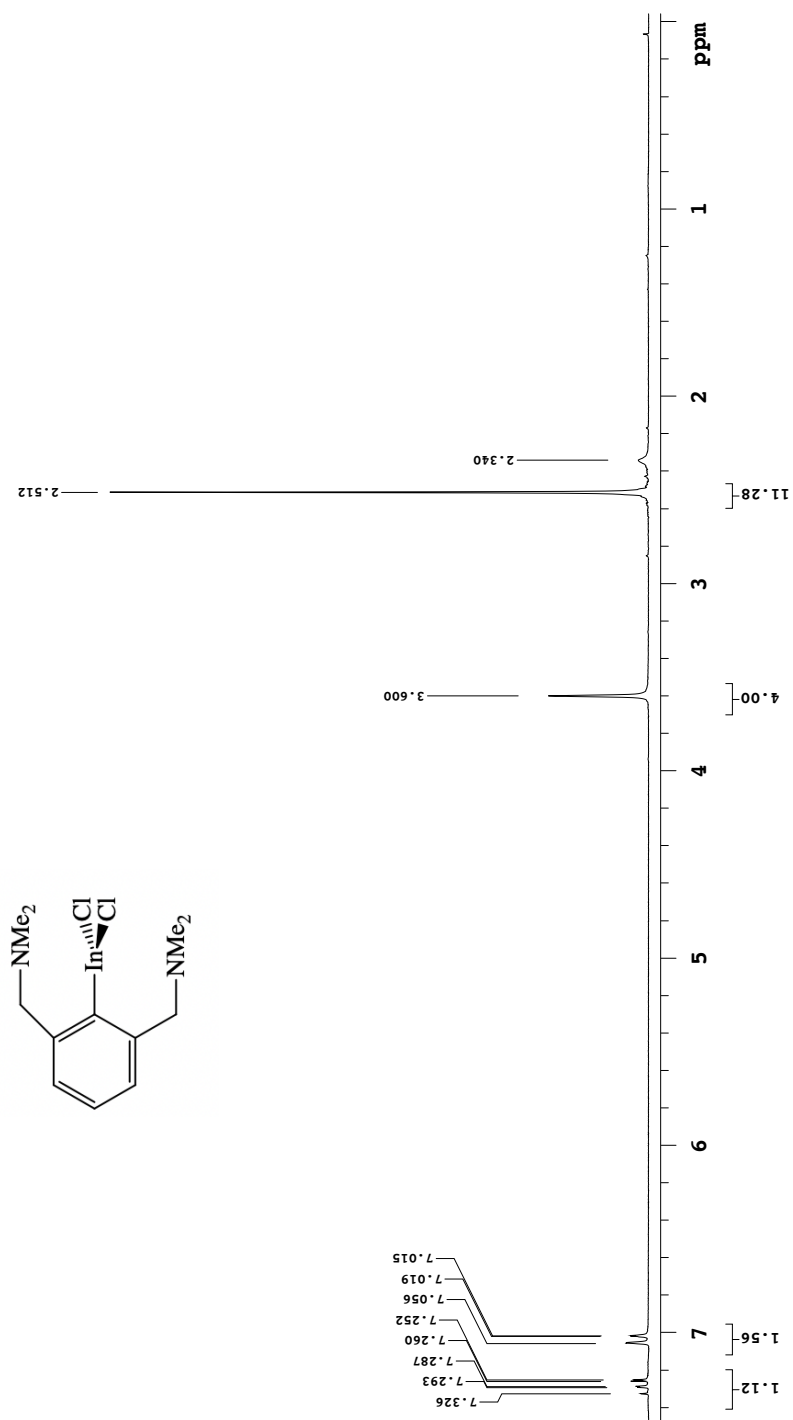


**Figure A.4:**  $^1\text{H-NMR}$  spectrum of  $(\text{NCN})\text{InCl}_2$  (**4**) in  $\text{CDCl}_3$ .

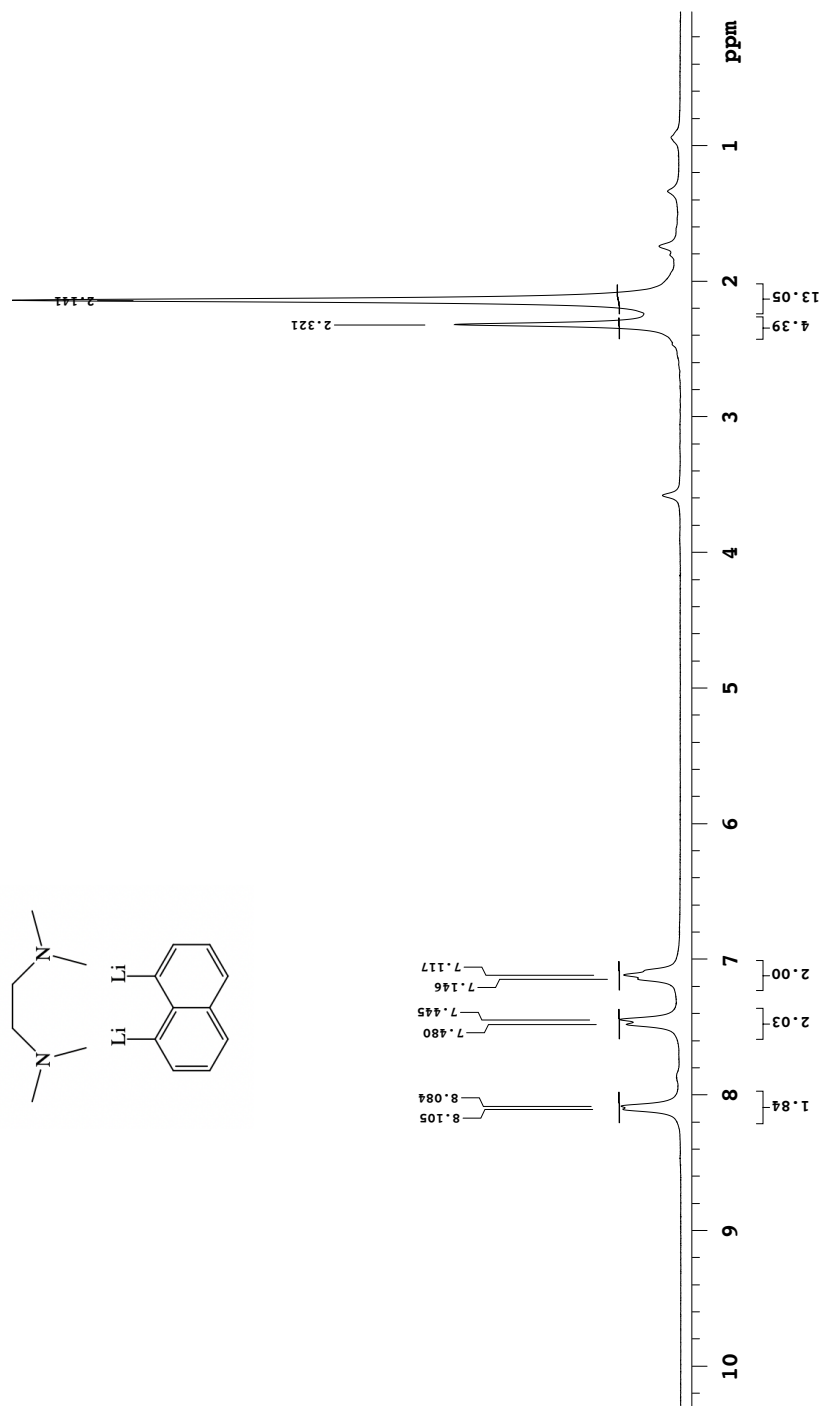


**Figure A.5:**  $^1\text{H-NMR}$  spectrum of  $\text{Li}_2(\text{naphth})(\text{TMEDA})$  (7) in  $\text{THF-d}_8$ .

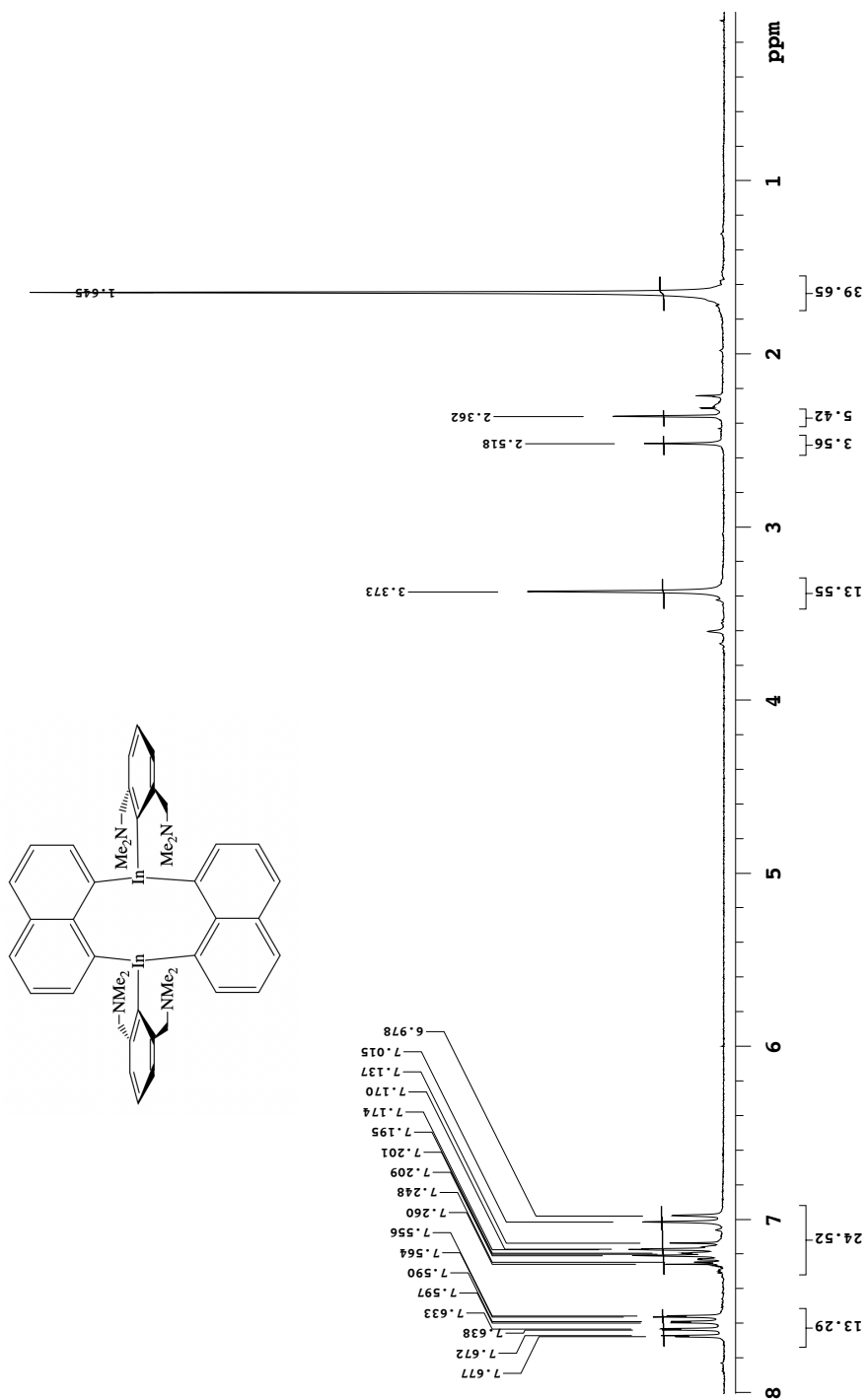


**Figure A.6:**  $^1\text{H-NMR}$  spectrum of  $[(\text{NCN})\text{In}]_2(\text{naphth})_2$  (**8**) in  $\text{CDCl}_3$ .

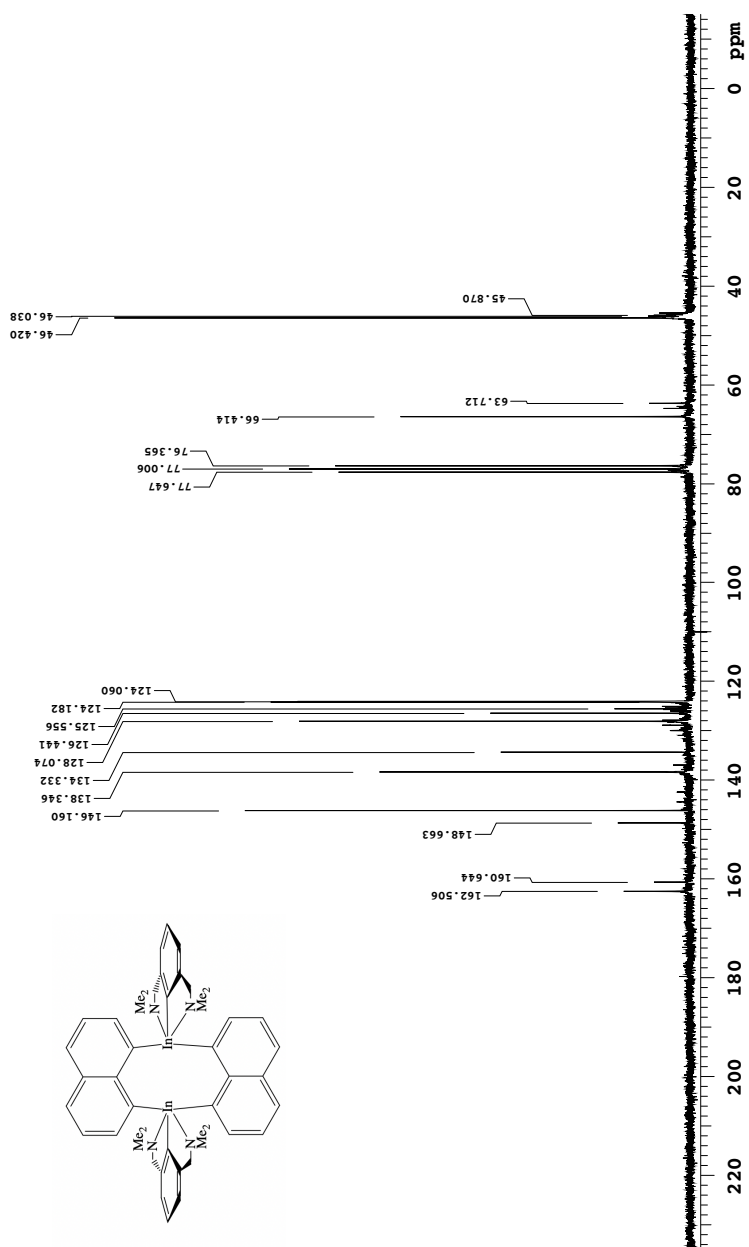


**Figure A.7:**  $^{13}\text{C}\{^1\text{H}\}$ -NMR spectrum of  $[(\text{NCN})\text{In}]_2(\text{naphth})_2$  (**8**) in  $\text{CDCl}_3$ .

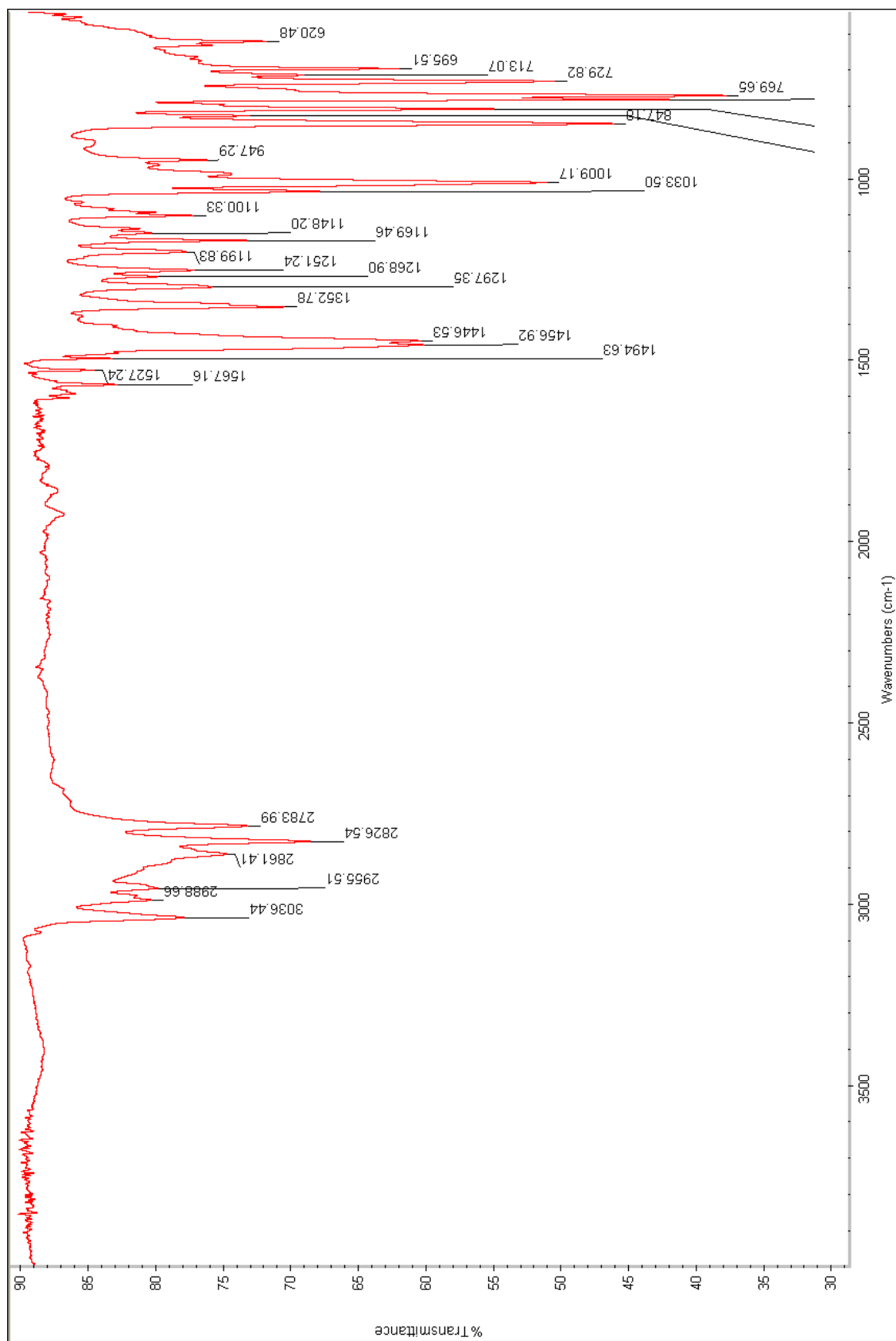
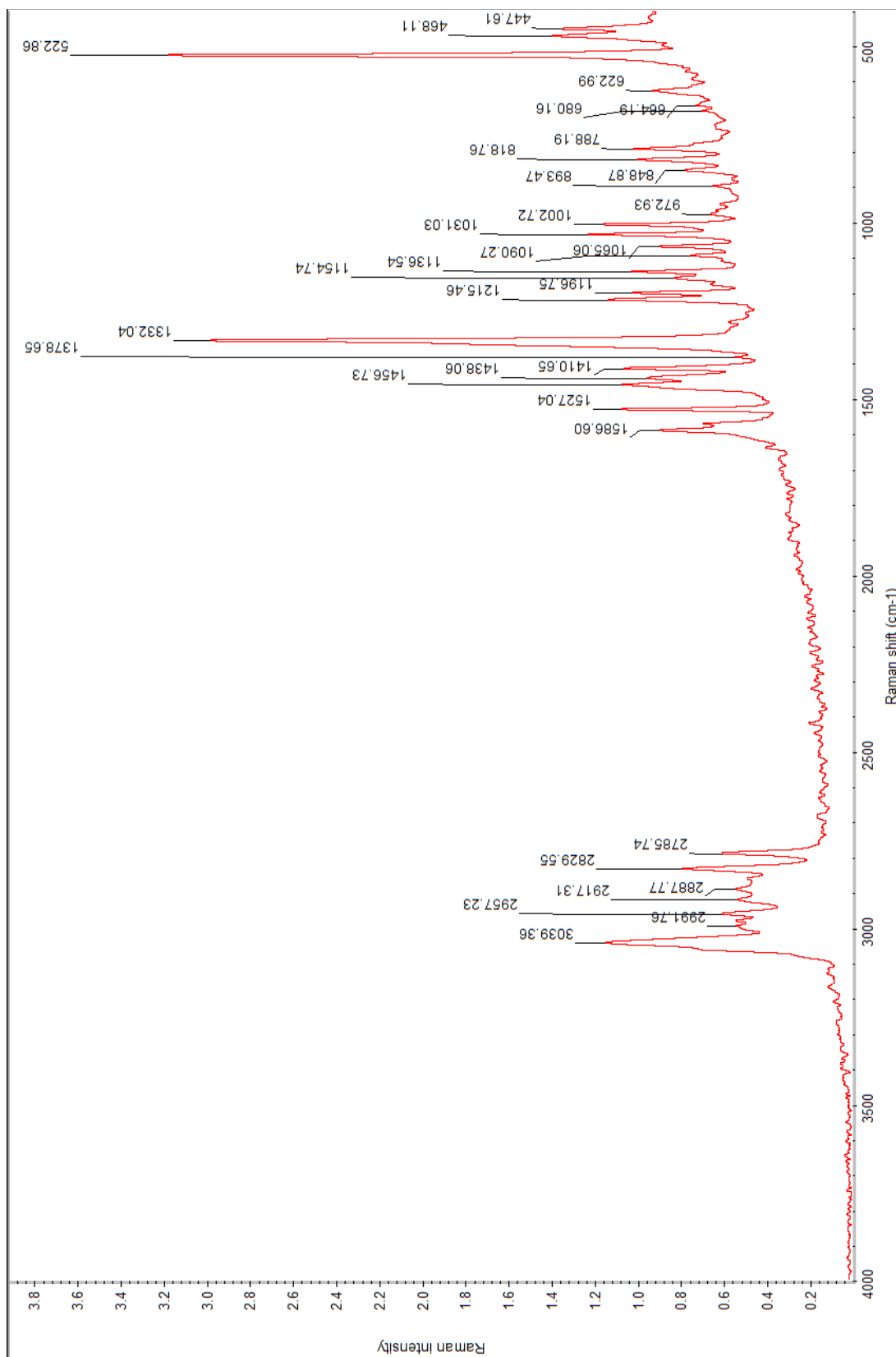


Figure A.8: FT-IR spectrum of  $[(NCN)In]_2(naphth)_2$  (8).



**Figure A.9:** FT-Raman spectra of  $[(\text{NCN})\text{In}]_2(\text{naphth})_2$  (**8**).

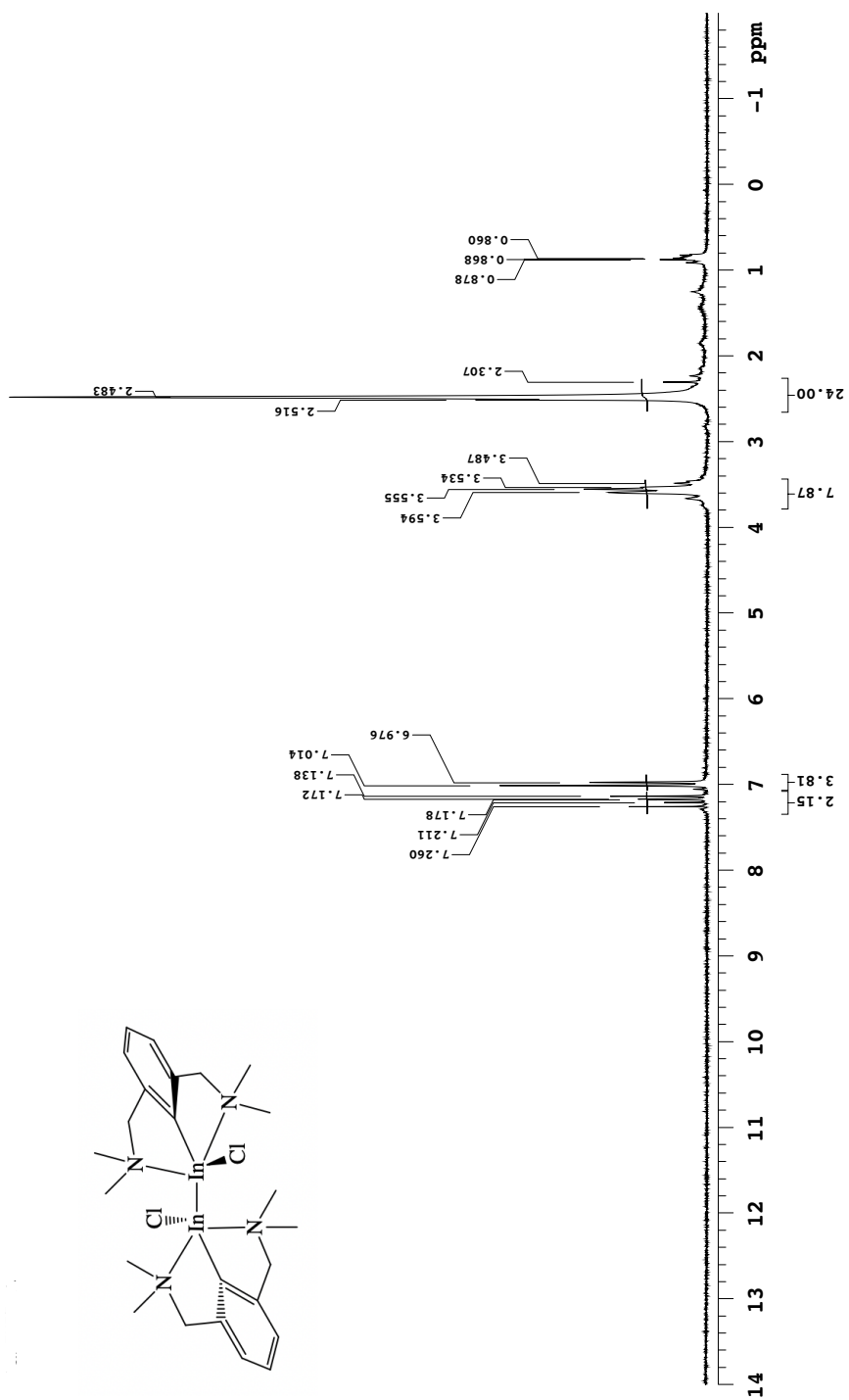


Figure A.10:  $^1\text{H-NMR}$  spectrum of  $[(\text{NCN})\text{InCl}]_2$  in  $\text{CDCl}_3$  (9).